WIND-INDUCED SEDIMENT RESUSPENSION AND ITS IMPACT ON ALGAL GROWTH FOR LAKE BALATON

R.A. Luettich, Jr.
University of North Carolina Institute of Marine Sciences, Morehead City, NC, USA

D.R.F. Harleman
R.M. Parsons Laboratory, Massachusetts Institute of Technology, Cambridge, MA, USA

L. Somlyódy and L. Koncsos
Water Resources Research Centre (VITUKI), Budapest, Hungary

RR-93-3
February 1993

INTERNATIONAL INSTITUTE FOR APPLIED SYSTEMS ANALYSIS
Laxenburg, Austria

Dynamic Behavior of Suspended Sediment Concentrations in a Shallow Lake Perturbed by Episodic Wind Events reprinted with permission from *Limnology and Oceanography* (1990) **35**(5):1050–1067.

Influence of Sediment Resuspension on the Light Conditions and Algal Growth in Lake Balaton reprinted with permission from *Ecological Modelling* (1991) **57**:173–192.

Printed by Novographic, Vienna, Austria.

Foreword

IIASA's joint study with the Hungarian Academy of Sciences (HAS) on eutrophication management of Lake Balaton was completed in 1982. The short-term control strategy worked out as a result of that study served as a basis for the governmental policy-making procedure which occurred in 1983. The study also identified future research needs. Wind-induced sediment resuspension and its impact on algal growth for shallow water bodies was considered as perhaps the most important one. The related research for Lake Balaton was then performed in the framework of a NSF/HAS project by the Water Resources Research Centre (VITUKI) and the Ralph M. Parsons Laboratory of MIT. (Both institutes were involved in the earlier IIASA study.) The present research report combines two journal articles which were published concerning the study. The first one, by Luettich, Jr. *et al.* (1990), deals with the understanding and modeling of physical processes influencing resuspension, while the second one, by Somlyódy and Koncsos (1991), builds on the achievements of Luettich, Jr. *et al.* and estimates the impact on light conditions and algae biomass. Due to an increased internal phosphorus load and the appearance of nitrogen-fixing blue-green algae, nowadays nutrients are not a limiting factor for Lake Balaton (in spite of the significant load reduction realized since 1983). The short-term dynamics of algae biomass are primarily determined by light, as described in the second article.

LÁSZLÓ SOMLYÓDY
Leader
Water Resources Project

Limnol. Oceanogr., 35(5), 1990, 1050–1067

Dynamic behavior of suspended sediment concentrations in a shallow lake perturbed by episodic wind events

Richard A. Luettich, Jr.
University of North Carolina Institute of Marine Sciences, 3407 Arendell St., Morehead City 28557

Donald R. F. Harleman
R. M. Parsons Laboratory, Massachusetts Institute of Technology, Cambridge 02139

Lâszló Somlyódy
Research Centre for Water Resources Development, Budapest, Hungary

Abstract

Field experiments were conducted in Lake Balaton, a large (surface area, 600 km^2) but shallow (mean depth, 3.2 m) lake in Hungary, to quantify the resuspension and deposition of bottom sediment due to episodic storm events. Measurements were made of windspeed and direction, surface waves, mean water velocity, and suspended sediment concentration. During significant wind events, the computed bottom stress due to surface waves dominated that due to the mean current, and therefore surface waves were assumed to be the major cause of sediment resuspension. A simple model for the depth-averaged suspended sediment concentration based on surface wave height was calibrated with about 10 h of data collected during one storm event and verified against 15 d of data collected at the same site. The success of the suspended sediment model, which assumes that the bottom sediment was noncohesive, is surprising since the bottom material was composed predominantly of sediment in the clay and fine-silt size ranges. This fit may indicate the presence of a thin surface layer of loosely bound sediment that is continuously involved in resuspension. The suspended sediment model could easily be integrated into a water quality model (e.g. to predict light attenuation), provided that lateral transport is negligible, or it could be used to provide the bottom boundary condition for a more general suspended sediment transport model in which advective transport is included.

Due to their small fall velocities, fine-grained particles (i.e. those in the silt and clay size ranges) are transported easily by flows. An understanding of the dynamic behavior of these particles is particularly important in shallow lakes and estuaries since there they may repeatedly settle to the bottom and be resuspended throughout the water column.

Lake Balaton, Hungary, is an example of a shallow body of water that is significantly affected by fine-grained suspended sediment. This lake has the largest surface area of any lake in central Europe (about 600 km^2) but has a mean depth of only 3.2 m (Fig. 1). A recent survey of the bottom sediment by Máté (unpubl.) has shown that it consists primarily of fine silt and clay except near the southern shore and in the Tihany Straits where coarser fractions prevail. The water quality in the lake is affected by resuspension and settling of these sediments in at least two ways. First, sediments suspended in the water column decrease light penetration, yielding Secchi disk depths that can be 20 cm or less and rarely are as much as 1 m. In the hypertrophic western end of the lake there is evidence that in summer light limits phytoplankton growth (Luettich and Harleman 1986). Second, the sediments are capable of acting as an internal

Acknowledgments

This work was supported jointly by the National Science Foundation and the Hungarian Academy of Science under the U.S.–Hungary Cooperative Science Program (grants INT 81-12454 and INT 84-11545) and by the National Science Foundation Environmental Engineering Program (grant ECE 82-11525).

Sandy Williams and Dick Koehler spent many hours making BASS work with the instrumentation system. The fieldwork at Lake Balaton would have been impossible without the help of many of the staff members at the Limnological Research Institute of the Hungarian Academy of Sciences and at the Hungarian Research Centre for Water Resources Development. Suggestions made by W. B. Dade, J. W. Lavelle, and an anonymous reviewer improved this paper and are acknowledged.

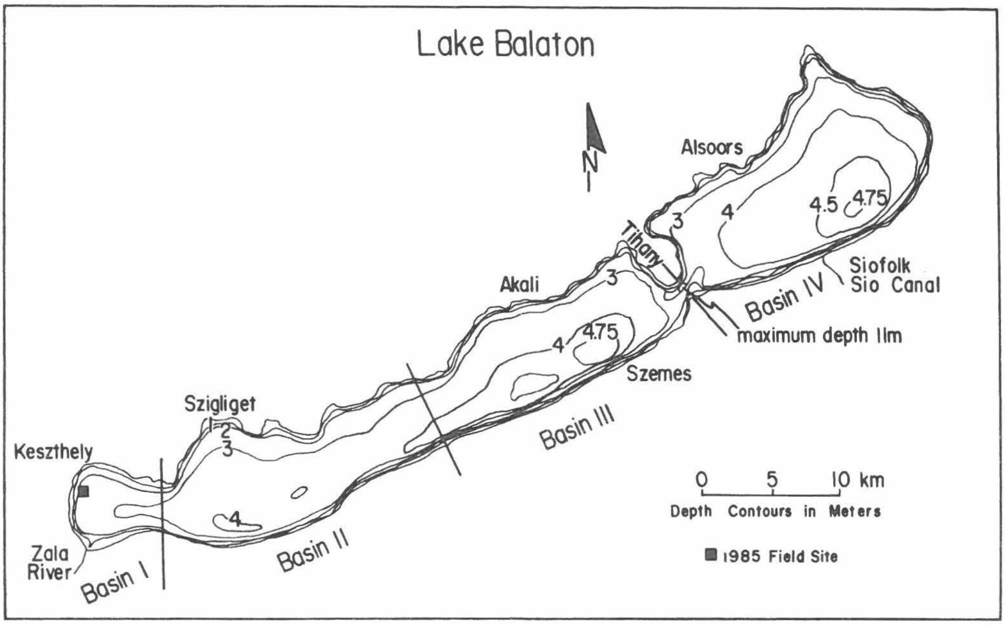

Fig. 1. Lake Balaton, Hungary.

source of nutrients because as much as 95% of the external supply of P to the lake is retained in the bottom sediments. Lijklema et al. (1986) found orthophosphorus concentrations in Lake Balaton sediments that were two orders of magnitude greater than in the overlying lake water. Experimental work by Gelencsér et al. (1982) showed that the desorption of P from bottom sediments resuspended by even a moderate storm could be comparable in magnitude to the daily average external supply. This internal source of nutrients may be particularly important to Lake Balaton, since in 1983 a comprehensive P reduction program was launched covering the entire watershed of the lake (Láng 1986).

As a component of a larger effort to address the effects of sediment on water quality in the lake (Somlyódy and van Straten 1986), the objective of the present study was to develop a model to predict storm-induced changes in the suspended sediment concentration of the lake. This paper presents the results of a field program to measure the hydrodynamic and sediment response of the lake to storm events and the development and application of a model for the suspended sediment concentration.

Field study

Instrumentation—A field study was conducted in water 2 m deep about 300 m from the western end of the lake (Fig. 1) from 6–21 August 1985. Suspended sediment concentrations were determined gravimetrically with middepth water samples collected from a boat anchored at the field site. Sampling was accomplished by lowering an empty 1-liter bottle to the desired depth and subsequently opening a vent tube that ran to the surface. This permitted water to enter the bottle through a sampling port as the air escaped through the vent tube. Samples were taken every 2–3 h during an initial storm and subsequent calm periods and as often as every 10 min during a second storm. Windspeed and direction were recorded continuously at a land-based meteorological station about 500 m from the site.

Additional data were collected from a tripod-based system of instruments that included windspeed and direction sensors mounted 2 m above the mean water level

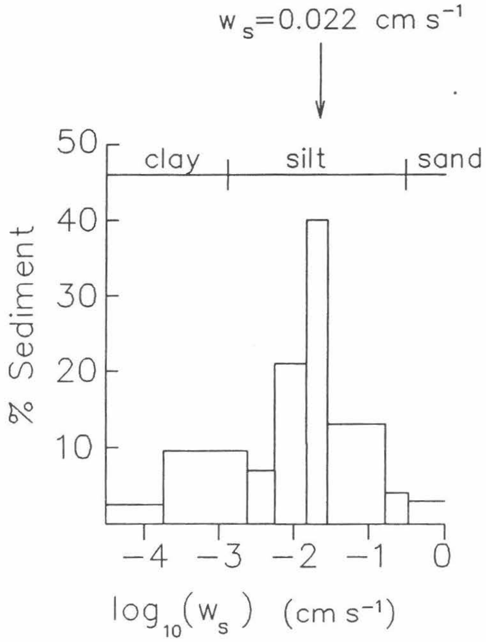

Fig. 2. Settling velocities of surface sediment collected at the field site.

and two BASS velocity meters located 24 and 85 cm above the bottom. BASS is an acoustic time-of-travel sensor that is capable of resolving water velocity in three dimensions to 0.03 cm s^{-1} (based on a 12-bit analog to digital conversion) and has an accuracy of 0.3 cm s^{-1} (limited by the repeatability of velocity measurements in still water) (Williams 1985). The distance from each BASS sensor to the bottom was measured in situ 5 d after the tripod was deployed and therefore accounts for initial tripod settling into the sediments. Subsequent measurements indicated that further settling was negligible.

A remote-control assembly that consisted of a C.B. radio and a tone-decoding circuit was mounted on the wind sensor mast. It allowed the instruments to be turned on and off and the sampling rate to be varied by sending different tone sequences over the radio.

Results—Settling-column analyses of bottom material collected by a diver indicated that the surface sediment consisted principally of clay and fine silt (Fig. 2). Plots of windspeed and direction from the meteorological station show that two major storms (beginning at about 0000 hours on 7 August and 2200 hours on 17 August) occurred during the study period. Each storm had northerly winds with hourly averaged speeds of 7–9 m s^{-1} (Fig. 3a). These events were responsible for increasing the middepth suspended sediment concentration from a background level of about 15 mg liter^{-1} to maximum concentrations >150 mg liter^{-1} (Fig. 3b).

Unfortunately, the tripod-based instruments could not be deployed until after the first storm. Also, many of the data collected while the instruments were deployed were lost due to a corroded connector between the data-logger housing and the housing containing the cassette tape used for data storage. Data were recorded successfully, however, for about 61 h from 2000 hours on 15 August to 0800 hours on 18 August, the final 10 h corresponding to the second storm. Data were collected at 2 Hz, although to conserve cassette tape they were taken in 6-min bursts once every hour, 30 min, or 15 min, depending on prevailing conditions.

Two small wind events during which the wind blew from east to west along the long axis of the lake were followed by the second major storm (Fig. 4a). Winds during the storm were oriented from north to south across the lake and were almost twice as strong as during the smaller events.

The vertical component of the velocity measured by the upper BASS was used to compute statistical wave properties. Extensive comparisons between the one-dimensional velocity spectra measured by the upper and lower BASS showed that linear wave theory accurately described velocities in the surface-wave band of the spectra for significant wave heights $\gtrsim$4 cm. Therefore linear theory was used to extrapolate vertical velocity spectra from the upper BASS into wave-height spectra at the surface. The wave-height spectra were then used to determine significant wave heights with assumptions for narrow-banded wave spectra (Ochi 1982). Reliable separation between wave velocities and turbulent velocities could not be obtained at significant wave

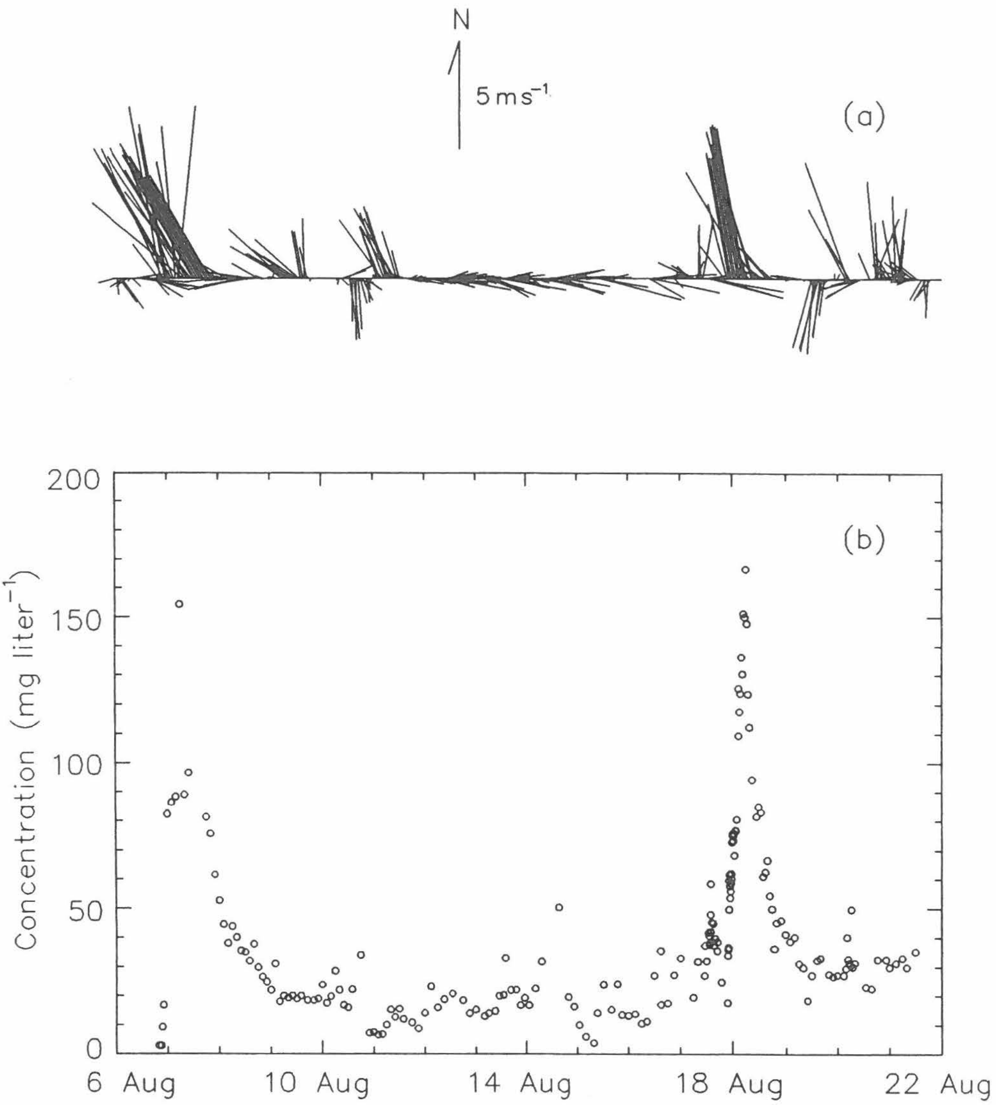

Fig. 3. a. The 30-min-averaged wind velocity measured at the Keszthely meteorological station during the 15-d field study. (Vectors point in the direction the wind is blowing from.) b. Observed middepth suspended sediment concentrations during the 15-d field study.

heights $\lesssim 4$ cm—therefore taken as a lower cutoff. During the two small events, significant wave heights reached ~ 17 cm, during the major storm they reached 25 cm (Fig. 4b). The mean period was relatively constant during each wind event at a value of ~ 2 s (Fig. 4c).

The current in the lower 85 cm of the water column was typically parallel to shore with maximal speeds of 10–12 cm s^{-1} (Fig. 5a,b). Although the two small wind events were similar in strength and direction, the corresponding horizontal water velocities were in opposite directions. It appears that in each case winds blowing along the lake enhanced the existing mean current at the

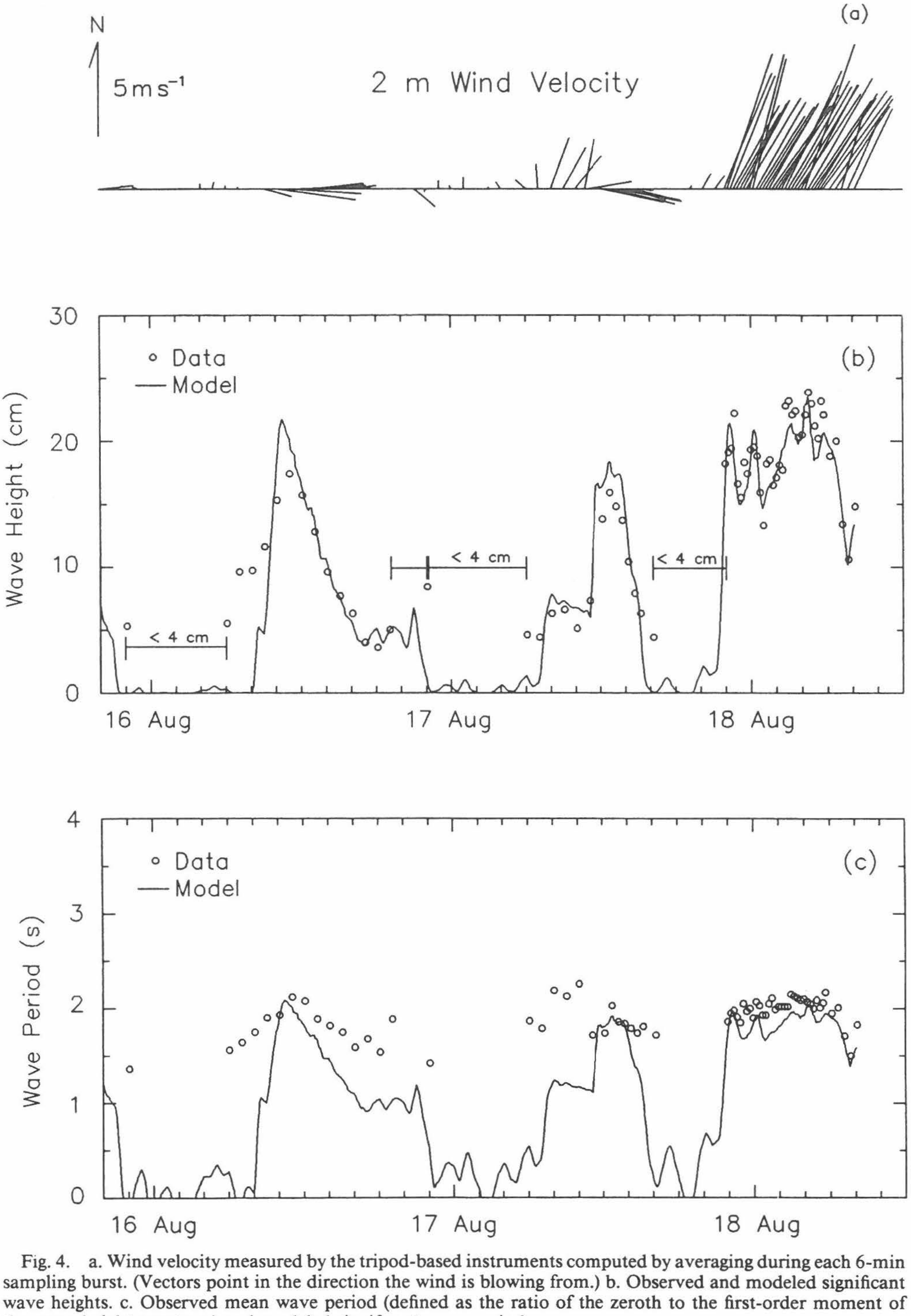

Fig. 4. a. Wind velocity measured by the tripod-based instruments computed by averaging during each 6-min sampling burst. (Vectors point in the direction the wind is blowing from.) b. Observed and modeled significant wave heights. c. Observed mean wave period (defined as the ratio of the zeroth to the first-order moment of the wave-height spectrum) and modeled significant wave period.

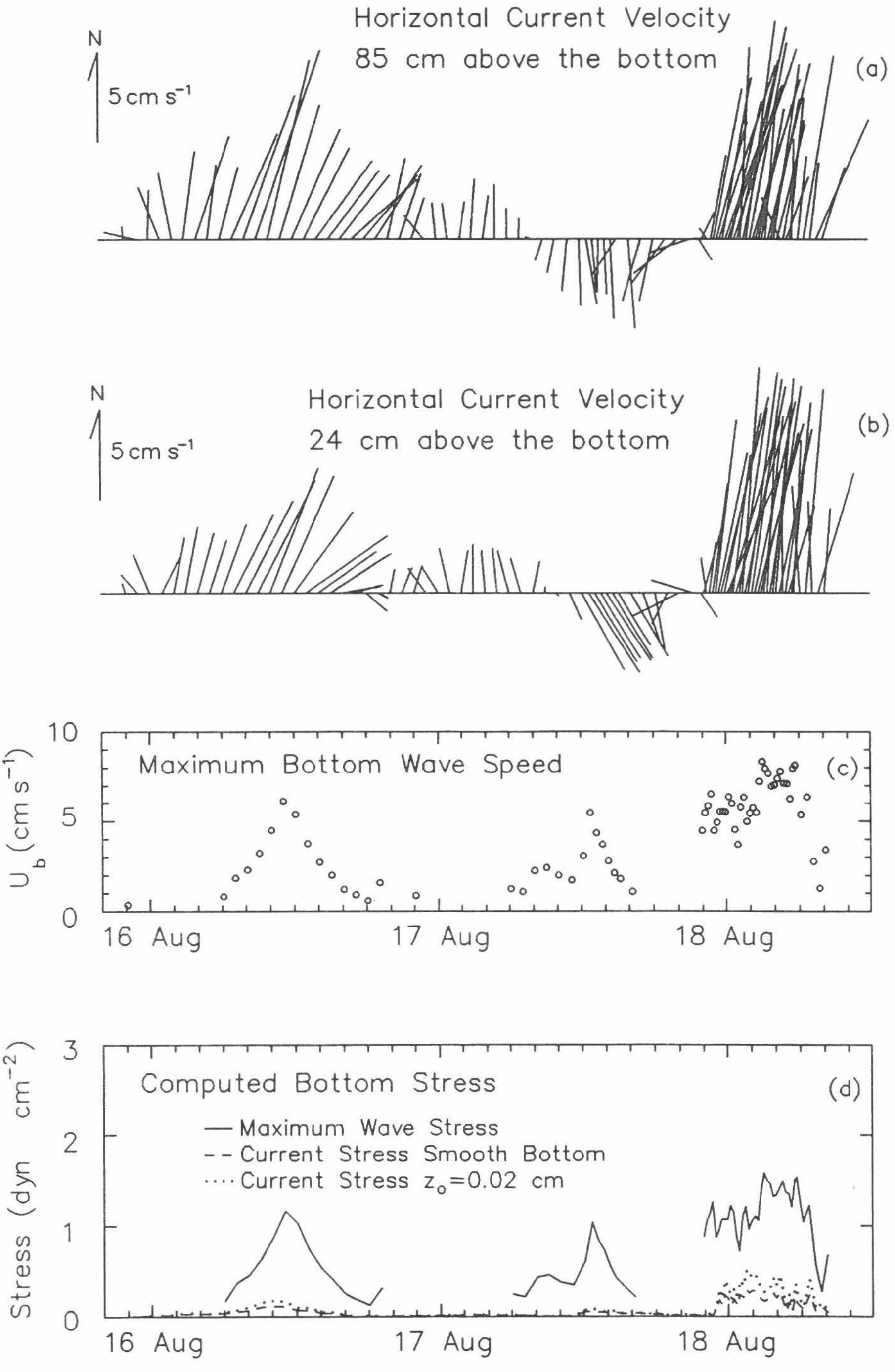

Fig. 5. a, b. Horizontal current velocity measured 85 and 24 cm above the bottom. (Vectors point in the direction the current is flowing toward.) c. Computed maximal, wave-induced orbital velocity at the bottom. d. Computed bottom stress due to the waves and current.

Significant symbols

A_b	Maximum bottom wave excursion amplitude (cm)
c	Suspended sediment concentration (mg liter^{-1})
$\bar{c}$, c_{bak}, c_e	Depth-averaged, nonsettling background, and equilibrium suspended sediment concentrations (mg liter^{-1})
E	Sediment pickup rate (g cm^{-2} s^{-1})
f_w	Wave friction factor
F	Effective fetch (m)
g	Acceleration of gravity (=9.81 m s^{-2})
h	Water depth (m)
H	Wave height (cm)
H_c, H_{ref}, H_s	Critical, reference, and significant wave heights (cm)
k	Wave number (m^{-1})
K	Model parameter (mg liter^{-1})
L	Length scale over which there is significant variation in c (km)
n	Model parameter
t	Time (s)
Re_w	Wave Reynolds number
T	Wave period (s)
T_c	Time scale for a significant change in c (min)
T_h	Horizontal transport time scale (h)
u, v, w	Water velocity components in the x, y, z directions
U	Mean advective velocity scale (cm s^{-1})
U_b	Maximum bottom wave orbital velocity (cm s^{-1})
$U_{curr}(z)$	Mean current velocity (cm s^{-1})
U_{*curr}	Mean current friction velocity (cm s^{-1})
w_s	Particle settling velocity (cm s^{-1})
W_{10}	Windspeed measured 10 m above the water surface (m s^{-1})
x, y	Horizontal coordinate directions
z	Vertical coordinate direction, positive upward, $z = 0$ at still water
z_0	Bottom roughness (cm)
α, ζ, γ, δ	Wave model constants
β	Model settling parameter (cm s^{-1})
Δt	Model time step (s)
κ	Von Kármán constant (=0.4)
λ	Wavelength (m)
ν	Kinematic viscosity of water (=0.01 cm^2 s^{-1})
ω	Wave frequency (s^{-1})
ρ	Density of water (=1 g cm^{-3})
τ	Bottom stress (dyn cm^{-2})
τ_c	Critical bottom stress (dyn cm^{-2})
τ_{curr}	Bottom stress due to mean current (dyn cm^{-2})
τ_{ref}	Reference bottom stress (dyn cm^{-2})
τ_{wave}	Maximum bottom stress during a wave cycle (dyn cm^{-2})
ϕ	Vertical sediment flux at the bottom (g cm^{-2} s^{-1})

measurement site. The direction of this current was probably determined by the seiching motion of the lake and by the previous wind history. During the major storm, the near-bottom current was directed toward the north, indicating a transverse setup in the lake, with a bottom return current against the wind.

Estimates of bottom stress due to the mean current and due to the surface waves were made to guide development of the sediment resuspension model. If the wave and current boundary layers are turbulent, the bottom stress is a highly nonlinear function of the near-bottom current velocity and the bottom wave orbital velocity (Smith 1977; Grant and Madsen 1979). Calculations for the 61 h of wave data indicate, however, that the wave boundary layer was probably viscous dominated (i.e. in the laminar regime as shown in Kamphius 1975, figure 9). In this case the wave and bottom stress can be treated separately.

The bottom stress associated with the mean current is

$$\tau_{curr} \equiv \rho U^2_{*curr}. \quad (1)$$

(Units given in list of symbols.) If the mean velocity profile is logarithmic near the bottom, U_{*curr} can be calculated from measurements of mean current velocity with

$$U_{*curr} = \frac{\kappa U_{curr}(z)}{\ln(z/z_0)}. \quad (2)$$

It was not possible to determine the hydraulic bottom roughness from the field measurements with adequate precision and therefore two estimates were used in Eq. 2, $z_0 = 0.02$ cm and $z_0 = \nu/9U_{*curr}$. The former value for z_0 is recommended over a mud bottom by Soulsby (1983) and is consistent with the value of $z_0 = 0.016$ cm obtained over a bottom of fine-grained sediment at the HEBBLE site during and after a storm (Gross et al. 1986). The latter value of z_0 comes from laboratory experiments over a smooth boundary (Monin and Yaglom 1971). Its use may be appropriate for our data because of the fine-grained bottom sediment and because daily dives at the field site revealed no discernible physically or biologically induced bedforms. τ_{curr} was calculated with the 6-min-averaged velocity measured by the lower BASS and therefore assumes that a logarithmic layer extended 24 cm above the bed.

Maximal bottom stress during a wave cycle can be computed as

$$\tau_{wave} = \frac{f_w}{2} \rho U_b^2. \quad (3)$$

(Summaries of Eq. 3–5 are found elsewhere: Sleath 1984; Dyer 1986.) In a viscous-dominated, wave boundary layer

$$f_w = 2(\mathrm{Re}_w)^{-1/2} \quad (4)$$

where Re_w is defined as

$$\mathrm{Re}_w \equiv \frac{U_b A_b}{\nu}. \quad (5)$$

It appears (Fig. 5d) that τ_{wave} dominates τ_{curr} by a factor ranging from 4 to 10, depending on which value of bottom roughness is used. The dominance of τ_{wave} over τ_{curr} occurs because bottom shear is proportional to the velocity gradient in the boundary layer. The current boundary layer has a characteristic period on the order of hours and therefore it can grow to a thickness comparable to the depth of the water column. Because surface waves have periods of only a few seconds, however, the wave boundary layer does not have a chance to grow to a thickness of more than a few millimeters. As a result the same bottom stress can be generated by wave-induced bottom orbital velocities that are much smaller than the mean current velocity. Since the bottom orbital velocity and the mean current velocity are typically of the same order of magnitude in Lake Balaton (e.g. Fig. 5a–c), it may be reasonable to neglect the stress due to the mean current in comparison with that due to the waves when specifying the forcing responsible for eroding bottom sediments. This conclusion is consistent with field data reported by Anderson (1972) for floodtides over a tidal flat, by Lesht et al. (1980) on the Long Island inner continental shelf, and by Carper and Bachmann (1984) in a small prairie lake—each of whom found that concentrations of fine particles in suspension were correlated with the presence of surface waves.

Suspended sediment model development

For conditions typically encountered in nature, the suspended sediment concentration can be modeled with a three-dimensional mass transport balance:

$$\frac{\partial \bar{c}}{\partial t} + \frac{\partial}{\partial x}[\overline{uc}] + \frac{\partial}{\partial y}[\overline{vc}] + \frac{\partial}{\partial z}[(\bar{w} - w_s)\bar{c}]$$

$$= -\frac{\partial}{\partial x}[\overline{u'c'}] - \frac{\partial}{\partial y}[\overline{v'c'}] - \frac{\partial}{\partial z}[\overline{w'c'}]. \quad (6)$$

Molecular diffusion terms in Eq. 6 have been dropped in comparison with their turbulent counterparts.

If the total suspended sediment concentration is modeled with a single mass transfer equation, w_s can be expected to vary as a function of time due to changes in the particle size distribution. Such changes may occur because of differential settling and flocculation/deflocculation in the water column. Alternatively, the total suspended sediment concentration can be broken up into different size classes, each of which has its own transport equation and w_s (e.g. *see* Hawley 1983; McLean 1985; Lick 1986). With this approach, differential settling is modeled explicitly while flocculation and deflocculation are treated by including source-sink terms in the transport equation for each size class.

In laboratory experiments Krone (unpubl. rep.) found that discrete particle settling occurred for mud taken from San Francisco Bay at suspended sediment concentrations <300 mg liter^{-1}. Similarly Lee et al. (1981) found that the effects of flocculation were small for suspensions of Lake Erie sediments in freshwater at concentrations <500 mg liter^{-1}, while van Leussen (1986) found no effect of flocculation for suspensions of kaolinite in freshwater at concentrations of 50 mg liter^{-1}. On the basis of these results, the effects of flocculation and deflocculation in the water column are expected to have a negligible effect on the size distribution of suspended particles in Lake Balaton. Due to a lack of data on temporal variations in the particle size distribution in the lake, the total suspended sediment concentration was modeled by a single equation with constant w_s.

Equation 6 can be simplified for use in the present study by considering time scales that pertain to the Keszthely field site. If we assume that horizontal advection dominates horizontal turbulent diffusion, a time scale for the horizontal transport of suspended sediment can be expressed as $T_h \sim L/U$. Based on the velocities presented in Fig. 5a,b and a circulation study done by Shanahan and Harleman (1982), it is assumed that away from Tihany Straits, $U \sim 5$ cm s^{-1}. L depends on spatial variability in the bottom sediment properties and the applied forcing. Bottom sediment properties typically vary on scales of 1–5 km and larger (Máté unpubl.). Principal forcing appears due to surface waves (Fig. 5d). Winds blowing from the north across the lake have fetches at the field site of about 2.5 km and therefore a value of $L \sim 1$ km might be appropriate. Due to the long fetch, waves generated by winds blowing along the long axis of the lake have $L \gg 1$ km. Györke (unpubl. rep.) made transects across Keszthely Bay during a storm and found less than a factor of two difference in suspended sediment concentration, suggesting that $L \gg 1$ km. Even with the most conservative value of L, we estimate that $T_h \sim 6$ h or more.

Most of the time-significant variations in the middepth suspended sediment concentration occur on time scales of $T_c \sim 30$ min (Fig. 3). Since $T_c \ll T_h$, these concentration changes must be due to vertical fluxes rather than horizontal advection. The only exceptions occur near the end of prolonged periods of settling which follow major resuspension events. With this possible limitation, the horizontal advective and diffusive transport terms are dropped from Eq. 6, leaving

$$\frac{\partial \bar{c}}{\partial t} + \frac{\partial}{\partial z}[(\bar{w} - w_s)\bar{c}] = -\frac{\partial}{\partial z}[\overline{w'c'}]. \quad (7)$$

Vertical profiles collected in Keszthely Bay by Györke (unpubl. rep.), near Szemes by Somlyódy (1982), and near Tihany by Luettich (1987) all indicate that suspended sediment concentrations are nearly uniform in the vertical. Physically, this pattern is due to the small particle sizes in suspension and the shallowness of the lake, which allows turbulence to penetrate easily throughout the depth. The lack of a significant vertical concentration gradient makes it convenient to model the depth-averaged suspended sediment concentration. Integrating Eq. 7 over the water column with the assumptions of a constant depth and no sediment flux at the free surface yields

$$h\frac{\mathrm{d}\tilde{c}}{\mathrm{d}t} = \phi \quad (8)$$

where $\tilde{c}$ and ϕ are defined as

$$\tilde{c} \equiv \frac{1}{h}\int_{-h}^{0} \bar{c}\,\mathrm{d}z \quad (9)$$

$$\phi \equiv -w_s\bar{c}\,|_{-h} + \overline{w'c'}\,|_{-h}. \quad (10)$$

The specification of this boundary condition is a major source of uncertainty for sediment transport studies. In the present model a parameterization for ϕ was selected that is similar to expressions used by others (e.g. Lam and Jacquet 1976; Sheng and Lick 1979; Somlyódy 1982; Aalderink et al. 1985; Lavelle et al. 1984). Defining

$$\beta \equiv \frac{w_s\bar{c}\,|_{-h}}{\tilde{c}} \quad (11a)$$

and

$$E \equiv \overline{w'c'}\,|_{-h} \quad (11b)$$

and substituting these into Eq. 10 gives

$$\phi = -\beta\tilde{c} + E. \quad (12)$$

The term $\beta\tilde{c}$ in Eq. 12 is the downward sediment flux due to settling. Equation 11a indicates that β is equal to the settling velocity multiplied by a factor that depends on the vertical distribution of sediment suspended in the water column. (For very small particles, <1 μm, the effects of Brownian motion should also be included in β, Lick 1982.) Since the suspended sediment concentration remains nearly uniform over depth in Lake Balaton, it is expected that $\beta \approx w_s$.

E is parameterized as a function of excess bottom stress.

$$E = 0 \qquad \tau < \tau_c \quad (13a)$$

$$E = \beta K\left(\frac{\tau - \tau_c}{\tau_{ref}}\right)^n \qquad \tau \geq \tau_c \,. \quad (13b)$$

τ_{ref} has been included to make the term in parentheses dimensionless.

There is no rigorous theoretical justification of the power law in Eq. 13b as the correct functional form for E. However, it does seem to adequately reproduce measurements of E for both cohesive and noncohesive sediments (*see* Lavelle et al. 1984; Lavelle and Mofjeld 1987; Luettich 1987). Defining

$$c_e \equiv 0 \qquad \tau < \tau_c \quad (14a)$$

$$c_e \equiv K\left(\frac{\tau - \tau_c}{\tau_{ref}}\right)^n \qquad \tau \geq \tau_c \quad (14b)$$

allows Eq. 12 to be written as

$$\phi = -\beta(\tilde{c} - c_e) \quad (15)$$

and therefore Eq. 8 becomes

$$\frac{d\tilde{c}}{dt} = -\frac{\beta}{h}(\tilde{c} - c_e). \quad (16)$$

From Eq. 16 it is clear that in this model the depth-averaged concentration is continuously driven toward an equilibrium value defined by Eq. 14a, b. Because τ is variable in time, c_e also varies in time.

The suspended sediment concentration rarely dropped below ~15 mg liter^{-1} during the 15-d measurement period (Fig. 3). This "background" concentration can be attributed to very small inorganic particles as well as various planktonic species that were at major bloom levels during the measurement period. To reflect this background in the model, a nonsettling background concentration was introduced into Eq. 16

$$\frac{d\tilde{c}}{dt} = -\frac{\beta}{h}(\tilde{c} - c_{bak} - c_e) \quad (17)$$

where c_{bak} = 15 mg liter^{-1}.

As discussed previously it seems appropriate to set $\tau \approx \tau_{wave}$ in Eq. 14a, b throughout much of the lake. If we use linear wave theory together with Eq. 3, 4, and 5, the maximal wave-induced bottom stress is linearly related to the wave height by

$$\tau_{wave} = H\left[\rho\frac{(\nu\omega^3)^{1/2}}{2\sinh kh}\right] \quad (18)$$

where $\omega \equiv 2\pi/T$ and $k \equiv 2\pi/\lambda$. For a constant ω, the substitution of Eq. 18 into Eq. 14a, b yields

$$c_e = 0 \qquad H < H_c \quad (19a)$$

$$c_e = K\left[\frac{H - H_c}{H_{ref}}\right]^n \qquad H \geq H_c. \quad (19b)$$

The wave period (and therefore ω) was relatively constant both during a wind event and from one wind event to another (Fig. 4c). Therefore we used Eq. 19a, b rather than Eq. 14a, b to determine c_e. A value of 1 cm was used as H_{ref}, which, with Eq. 18 and assuming $T = 2$ s and $h = 2$ m, is equivalent to $\tau_{ref} = 0.072$ dyn cm^{-2}.

If c_e is constant in time, Eq. 17 has the analytical solution

$$\tilde{c} = c_e + c_{bak} + (\tilde{c}_i - c_e - c_{bak}) \cdot\exp\left[\frac{-\beta}{h}(t - t_i)\right] \quad (20)$$

where the initial conditions are $\tilde{c} = \tilde{c}_i$ at $t = t_i$. The solution of Eq. 17 for a time-varying c_e can be obtained from Eq. 20 with a convolution integral if c_e varies smoothly or with a convolution sum if c_e varies discretely. In the present work it was assumed that c_e varied discretely in steps of length Δt. For each time step an average value of H was determined and used to calculate a value of c_e (Eq. 19a, b). Equation 20 was then used to determine the variation of $\tilde{c}$ over the time step taking $\tilde{c}$ and t from the end of the previous time step as $\tilde{c}_i$ and t_i. The resulting solution is identical to that obtained via a convolution sum and is much easier to implement. All of the model results presented below use Δt = 1,800 s. Sensitivity studies indicated that smaller values of Δt did not alter the solution significantly.

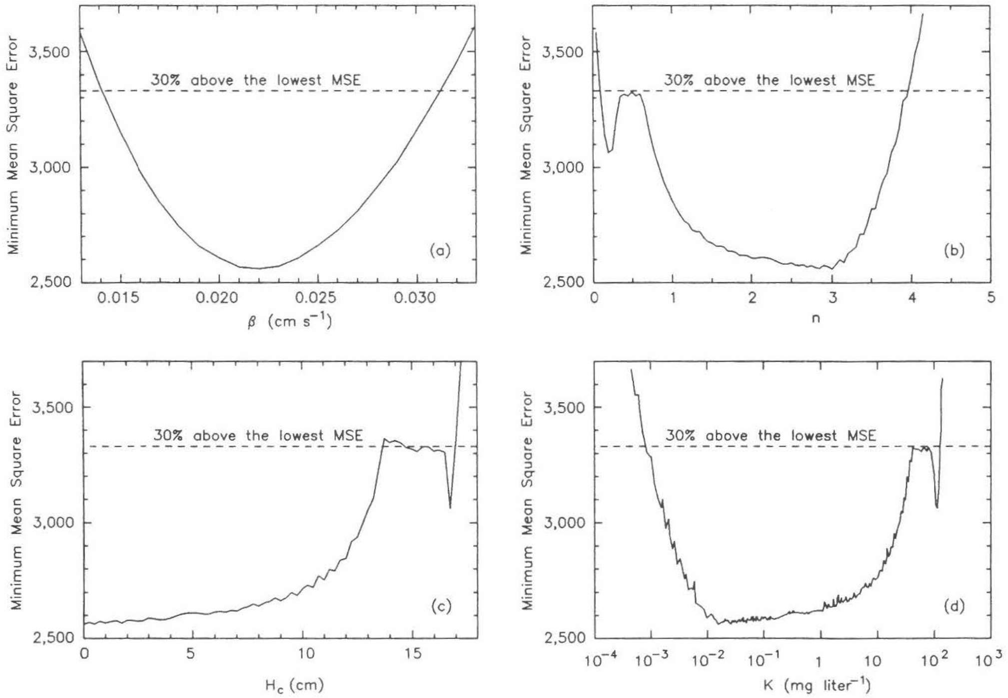

Fig. 6. Minimal MSE as a function of each calibrated parameter when all are allowed to vary independently. (For example panel a shows a projection onto the β-MSE plane of the lower envelope of the minimal MSE surface that exists in four-parameter space. The result is a curve of the minimum MSE as a function of β for all possible combinations of K, n, and H_c.) Horizontal lines represent MSE that is 30% above the lowest value found.

Model calibration and verification

Calibration of the suspended sediment model—The model was calibrated with the significant wave heights and suspended sediment concentrations measured during the second major storm. To do so it was assumed that the middepth measurements were representative of depth-averaged concentrations. The concentration 17.6 mg liter^{-1} measured at 2145 hours on 17 August was used as the initial condition. Calibration began by systematically and independently varying the parameters K, H_c, β, and n over a wide range of possible values and recording the sum of the mean square error (MSE) between the model predictions and the observed suspended sediment concentrations. Plots of the minimum MSE as a function of each parameter have a well-defined range of parameter values for which the minimum MSE curve is relatively flat (Fig. 6). Although it might be tempting to select the single parameter set which gave the lowest MSE and call it the optimal model calibration, doing so would ignore any error in the observed data and the fact that the model is only an approximate representation of the system. To allow for these errors, we considered all parameter sets giving MSE values within 30% of the lowest MSE equally acceptable (Table 1). This range

Table 1. Acceptable parameter combinations from model calibration.

MSE	2,560–3,330* mg^2 liter^{-2}
H_c =	0.0–16.8 cm
β =	0.015–0.031 cm s^{-1}
n =	0.15–3.95
K =	0.00086–125 mg liter^{-1}

* 30% variation from the lowest MSE. Specific parameter combinations within the listed ranges yield mean square errors between 2,560 and 3,330.

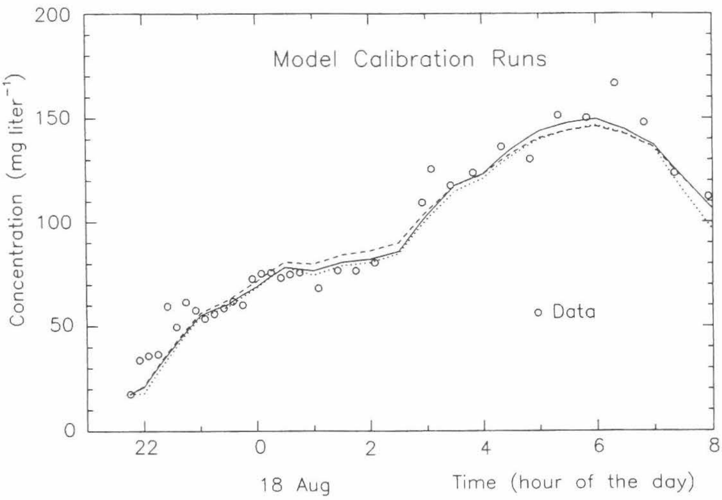

Fig. 7. Comparison between the model and calibration data for three parameter sets. Solid line—$n = 3$; $K = 0.0151$ mg liter^{-1}; $\beta = 0.022$ cm s^{-1}; $H_c = 0$ cm; MSE = 2,560 mg^2 liter^{-2}; dashed line—$n = 1.75$; $K = 1.19$ mg liter^{-1}; $\beta = 0.022$ cm s^{-1}; $H_c = 5.92$ cm; MSE = 2,820 mg^2 liter^{-2}; dotted line—$n = 0.88$; $K = 23.5$ mg liter^{-1}; $\beta = 0.022$ cm s^{-1}; $H_c = 13.4$ cm; MSE = 3,330 mg^2 liter^{-2}.

in MSE was selected arbitrarily and is meaningful only because it includes all parameter values in the flat parts of the curves in Fig. 6. Calibrations with larger and smaller acceptable ranges in MSE yielded increased and decreased limits on the acceptable parameter sets, respectively, but did not significantly affect the parameter covariances.

The wide range of acceptable parameter values (Table 1) indicates either that the model is insensitive to variations in one or more of the parameters or that too many degrees of freedom exist in the model. If it is assumed that $\beta \approx w_s$, however, the values of β are in excellent agreement with the measured settling velocities (Fig. 2). If we assume Stokes' settling law, they correspond to particles in the fine silt size range. To further examine the issue of degrees of freedom, we made a search for covariances between different pairs of parameters from among all of the parameter sets that gave acceptable model calibration. This showed that β was not correlated with any of the other parameters. Therefore a single value could be chosen for β without biasing any of the other parameter values. An average value of $\beta = 0.022$ cm s^{-1} was selected and used in final model runs. On the other hand, n and K were correlated through the relationship

$$n = -0.67 \log_{10}(K) + 1.8 \qquad r^2 = 0.987. \quad (21)$$

A second set of calibration runs was then made with $\beta = 0.022$ cm s^{-1} and K determined by Eq. 21. From the resulting acceptable parameter sets it was found that n and H_c were correlated through the relationship

$$\log_{10}(n) = -0.040H_c + 0.48 \qquad r^2 = 0.996. \quad (22)$$

If $\beta = 0.022$ cm s^{-1} and Eq. 21 and 22 are substituted into Eq. 20, one free parameter remains that cannot be assigned a unique value from the calibration data. Rather, acceptable model calibrations are obtained for a range of parameter values. Visually, these calibrations are nearly indistinguishable (Fig. 7).

Verification of a wave model—The application of the suspended sediment model requires information about surface waves. A simple model was developed to provide this information (Luettich and Harleman in press) with the shallow-water modifications

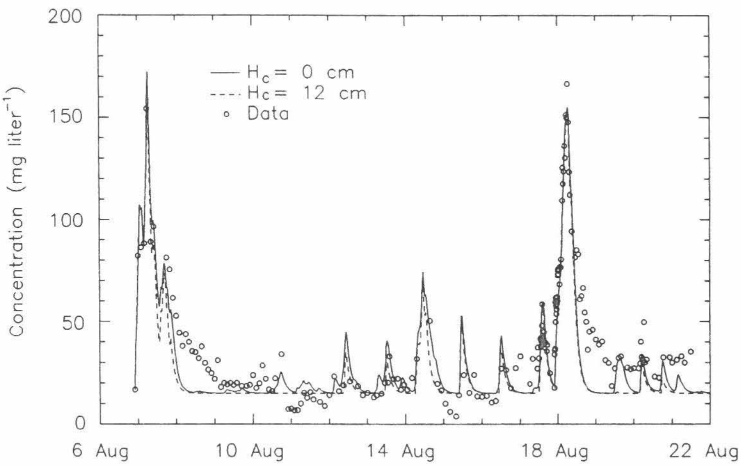

Fig. 8. Comparison between observed suspended sediment concentrations and the model predictions during the 15-d field study.

to the SMB method presented by the CERC (1974). The significant wave height and period are given for fetch-limited waves by the empirical equations:

$$\frac{gH_s}{W_{10}^2} = 0.283 \tanh[\alpha]\tanh\left[\frac{\gamma}{\tanh \alpha}\right] \quad (23)$$

$$\frac{gT}{W_{10}} = 2.8\pi \tanh[\zeta]\tanh\left[\frac{\delta}{\tanh \zeta}\right] \quad (24)$$

$$\alpha = 0.530(gh/W_{10}^2)^{1.75}, \quad (25a)$$

$$\zeta = 0.833(gh/W_{10}^2)^{1.375}, \quad (25b)$$

$$\gamma = 0.0125(gF/W_{10}^2)^{1.42}, \quad (25c)$$

$$\delta = 0.077(gF/W_{10}^2)^{1.25}. \quad (25d)$$

The effective fetch F is defined in the CERC (1974) publication. To use Eq. 23–25 it was assumed that the waves were in local equilibrium with the wind, i.e. that they traveled in the direction of the wind and that the local depth was appropriate for use in Eq. 25a, b. This assumption is reasonable throughout much of the lake because of the gradual changes in water depth. Windspeeds were adjusted up to the required 10 m by assuming a logarithmic velocity profile and using the drag coefficient formula suggested by Wu (1982).

Observed wave heights are reproduced quite well during the two early periods when the winds were blowing along the lake's long axis and during the storm when the winds were oriented across the lake (Fig. 4b,c). The slight overestimation near the beginning of the two events aligned with the lake's long axis suggests that the waves were initially duration rather than fetch limited. During the storm the unsteady nature of the observed wave heights is reproduced reasonably well by the model due to the short cross-lake fetch and therefore the short time required to reach fetch-limited conditions.

Unfortunately, the wave periods were not as well predicted. In order to make the predicted period match the observed period during the main part of each wind event, the leading coefficient in Eq. 24 was adjusted from its value of 2.4 in the original publication (CERC 1974) to 2.8. A more significant problem was that the observations tended to remain nearly constant at a period of about 2 s while the model showed much more variability. From this standpoint a more accurate representation of the observations is obtained by assuming a constant period equal to the average value predicted by the model during the main part of each wind event. Therefore Eq. 19a, b were used rather than 14a, b to model the suspended sediment data.

Verification of the suspended sediment model—The suspended sediment model was verified with a 15-d record of wind and suspended sediment data (Fig. 3). The wave model was used to convert wind velocities into wave heights for the suspended sediment model. The concentration 16.75 mg liter^{-1} measured at 2200 hours on 6 August was used as the initial condition. H_c was chosen to be the model's free parameter. In general the model does a good job of reproducing observed suspended sediment concentrations during the two major storms, which were oriented across the lake, and during many of the smaller wind events, which were typically oriented along the lake (Fig. 8, Table 2). As indicated in Table 2, a MSE range within 30% of the lowest value can be obtained with H_c varying from 0 to 13 cm. Over the range of H_c from 0 to 8 cm, the model results are nearly indistinguishable, and the MSE varies by <1.5%.

The only systematic deviations between the model and the observations follow the two major storms, when predicted concentrations decrease more rapidly than observed concentrations. As discussed previously, horizontal transport was neglected in the model and therefore may be an explanation for the discrepancy since a relatively long period is associated with particle settling. Györke (unpubl. rep.) found less than a factor of two difference in suspended sediment concentrations across Keszthely Bay during a storm, however, which suggests that the effects of horizontal transport should be small. A more likely explanation for the model discrepancy is differential settling. Because larger particles settle faster than smaller ones, the average settling velocity should decrease during prolonged periods of deposition. This time variation is exactly what the observations appear to show. We note that if a reduced settling rate is taken into account, the model agrees more closely with observations even during several small wind events that occur shortly after each major storm.

Because it was not possible to select a single value for each of the model parameters from either the calibration or verification data sets, several efforts were made to extrapolate values from the literature.

Table 2. Summary of results for varying H_c with verification data.

H_c (cm)	c_{bak} (mg liter^{-1})	β (cm s^{-1})	n—Eq. 22	K—Eq. 21 (mg liter^{-1})	MSE (mg^2 liter^{-2})
0.0	15	0.022	3.02	0.0148	34,400
2.0	15	0.022	2.51	0.0855	34,400
4.0	15	0.022	2.09	0.368	34,300
6.0	15	0.022	1.74	1.24	34,300
8.0	15	0.022	1.45	3.40	34,800
10.0	15	0.022	1.20	7.88	37,000
12.0	15	0.022	1.00	15.9	40,500
13.0	15	0.022	0.91	21.5	43,800
14.0	15	0.022	0.83	28.3	48,200

Stokes' settling law gives $w_s = 0.022$ cm s^{-1} for a particle diameter of 16 μm. Extensions of Shields' curve for small particles by Mantz (1977) and Miller et al. (1977) suggest a critical stress of $\tau_c \sim 0.5$ dyn cm^{-2}. Using Eq. 18 and assuming waves of 2-s periods gives $H_c \sim 7$ cm—well within the range of values for which the model is calibrated.

Alternatively Lavelle et al. (1984) and Lavelle and Mofjeld (1987) argued that τ_c (and therefore H_c) should be zero. Their arguments are based on the highly subjective way in which critical stresses have been determined in laboratory experiments, the stochastic nature of bottom stresses and particle movement, and the fact that previous experimental results, which were originally interpreted with a nonzero critical shear stress, can also be represented with $\tau_c = 0$. For the present model the choice of $H_c = 0$ is clearly consistent with the model calibration (*see Fig. 6c*) and with the model verification.

Assuming $\tau_c = 0$, Lavelle et al. (1984) reanalyzed erosion rates obtained from several laboratory experiments with fine-grained sediments and found values of n ranging from 1.2 to 5 and values of the rate coefficient ranging from 1.9×10^{-9} to 3.7×10^{-6} g cm^{-2} s^{-1}. Using $H_c = 0$ in Eq. 21 and 22 gives $n = 3.0$ and $K = 0.015$ mg liter^{-1}. Substituting into Eq. 13b along with $\tau_{ref} = 0.072$ dyn cm^{-2} yields

$$E = 3.3 \times 10^{-10}(\tau/\tau_{ref})^3 = 9 \times 10^{-7}\tau^3 \text{ g cm}^{-2}\text{ s}^{-1}. \qquad (26)$$

Both the exponent $n = 3$ and rate coefficient fall within the ranges found by Lavelle et al. (1984), confirming that $H_c = 0$ is also a plausible result.

In summary, the calibration and verification results suggest that it is possible to successfully model the transient behavior of the suspended sediment concentration at our field site with the boundary condition expressed in Eq. 12 and 19. Due to the form of this boundary condition, however, if a small range is allowed in acceptable model behavior, a rather large range can be obtained in acceptable model parameters. We anticipate that a similar conclusion would also apply to the analysis of data from laboratory studies of fine sediment erosion. Therefore it is not surprising that Lavelle et al. (1984) and Lavelle and Mofjeld (1987) were able to fit laboratory experiments with erosion expressions having $\tau_c = 0$ that were originally interpreted with a nonzero τ_c.

The role of cohesiveness in the suspended sediment model

The measured particle settling velocities along with the muddy character of the bottom suggested that the sediments at the study site would be cohesive and therefore that the parameterization used to close Eq. 10 should reflect this property. For convenience, cohesion is generically used to describe both cohesive and adhesive bonding between particles.

Laboratory studies have shown that the erosion and deposition of cohesive sediments are different and exclusive processes. Erosion occurs from a cohesive sediment bed until the depth is reached where the bed strength is equal to the erosive force (Mehta and Partheniades 1979). The bed strength depends on the amount of consolidation that has occurred since the bed was deposited, the make-up of the bed, the temperature, the chemistry of the overlying water and the pore fluid, and bioturbation and secretions by benthic organisms (Southard et al. 1971; Fukuda and Lick 1980; Lee et al. 1981; Parchure and Mehta 1985). Deposition takes place when the applied stress is unable to resuspend or break apart particles or flocs that settle to the bed. It depends on the initial concentration of sediment in suspension, the physicochemical properties of the sediment in suspension, and the applied stress (Mehta and Partheniades 1975).

Sediment cohesiveness can be included in the bottom flux boundary condition, Eq. 15, via the appropriate definition of c_e (Luettich 1987). In this case, however, c_e will depend on the cohesiveness of the sediment bed and therefore its magnitude (for the same applied stress) will vary in time as the bed consolidates. In addition its functional form will be different depending on whether the bed is eroding or accumulating.

In the model results presented above, c_e was determined by an expression whose form and parameters remained constant in time. As a result, the sediment was being treated as if it were noncohesive. Yet, there were no indications from model behavior that this treatment was unsatisfactory. Although it might be possible that the omission of cohesive effects caused the deviation between the model and the observations during poststorm deposition periods, this interpretation seems unlikely because the model matched the observations quite closely during the initial stages of deposition. Only after 60% or more of the sediment had left suspension did the discrepancy occur.

As a result, the following paradox is suggested: the sediment character suggests that it was cohesive, but the suspended sediment concentration could be modeled as if the sediment was noncohesive. We note that the same paradox applies to the work of Lam and Jacquet (1976), Sheng and Lick (1979), Somlyódy (1982), Aalderink et al. (1985), and Lavelle et al. (1984), all of whom modeled sediment that was presumably cohesive with boundary conditions which treated it as noncohesive.

One explanation is that all of the models simply do a good job of curve fitting. Since it is not our purpose here to assess the success of the other models, our remarks are restricted to the present model. As developed and applied in the preceding sections, the present model is closely based on the physics of the system and has relatively few adjustable parameters. These parameters have been objectively calibrated and verified with independent data sets, with the verification data including winds blowing both across and along the axis of the lake. The calibrated value of β is in excellent agreement with expected values of w_s based on the particle size distribution, and the resulting parameter values agree with those obtained from laboratory measurements of fine sediment erosion. The only systematic deviation between the model and observations is plausibly explained by differential settling which is not included in the model. Therefore, we feel that the present model does more than coincidentally represent the system behavior.

Another explanation is that the sediments do behave as if they are noncohesive. We speculate that this behavior is the result of a thin layer of sediments that exists at the surface of the sediment bed and whose contents never become cohesively bound to the bed. The thickness of this noncohesive layer may be very small since a suspended sediment concentration of 200 mg liter^{-1} in a 2-m water column can be obtained by suspending an 0.8-mm-thick sediment layer that has a 95% water content. Possible mechanisms for keeping this layer from becoming part of the bed include bioturbation due to benthic animals and shear associated with the mean current. Although the latter is small in comparison with that due to the waves, it remains relatively constant in time due to the continuous seiching motion of the lake. Also, there may be times that wave action is enough to agitate the surface sediment but not strong enough to resuspend it into the water column. Drake and Cacchione (1986) have found that observations of fine sediment resuspension in Norton Sound, Alaska, and on the northern California shelf also suggest the presence of a surface layer of cohesionless sediment.

Conclusions

The results of the field investigation carried out in Lake Balaton show that episodic increases in the suspended sediment concentration are forced by wind-generated surface waves. Although data were presented from only one field site, the shallowness of the entire lake and the generally comparable magnitude of wave-induced bottom orbital velocities and mean current velocities suggests that the results will generalize to much of the lake. The most probable exception would occur near Tihany Straits, where large mean currents are known to exist.

Assuming a local equilibrium between wind and waves, it was possible to do a good job of modeling significant wave heights at the field site with a fetch-limited model based on the shallow-water modifications to the SMB method presented by the CERC (1974). This model was not as successful at predicting wave periods, although it did give a reasonable average wave period during substantial wind events. Due to the gradual bottom slope of the lake, it is expected that this model can be used throughout much of the lake.

Observed middepth suspended sediment concentrations could be predicted at the field site over the 15-d study period with a model for the depth-integrated suspended sediment concentration. The model neglected vertical variations in the suspended sediment concentration, horizontal transport, and temporal variations in the particle size distribution and assumed that wave-induced bottom stress was the principal forcing for sediment resuspension. A calibration of the four model parameters to 10 h of data collected during the second major storm yielded ranges of acceptable parameter values comparable with those obtained from laboratory settling velocity measurements and previous laboratory studies of fine sediment erosion. After removing parameter covariances, one free parameter remained in the model for which a definitive value could not be selected based on the calibration data, the 15-d data set used for model verification, or information available in the literature.

The relatively small variation in model results for a large variation in parameter values is consistent with the results of Lavelle et al. (1984) and Lavelle and Mofjeld (1987) who were able to fit expressions having zero critical stress to data that had previously been interpreted with a nonzero critical stress. For this reason we recommend not using modeled suspended sediment concentrations as a basis for determining values of critical stress.

It is often suggested that the inability to determine a single set of parameter values, as experienced above, indicates that a model contains too many parameters and therefore that one or more parameter can be eliminated. It is not clear, however, in the present case that this suggestion is valid. The elimination of H_c is equivalent to setting it equal to zero. Since $H_c = 0$ may not be physically reasonable, the present model was left with the free parameter. The only systematic model deviation from observed data was toward the end of periods of prolonged deposition and was most likely caused by omission of differential settling from the model.

It was possible to do a good job modeling the suspended sediment concentration assuming that the sediment was noncohesive despite the fact that the sediment characteristics suggested otherwise. We speculate that while the major portion of the sediment bed may be cohesive, a thin layer of sediment particles exists at the bed surface that is kept from becoming part of the bed by bioturbation and bottom shear exerted by the mean current and small waves. Although the latter may be weak in comparison to the stress necessary to cause resuspension, it is almost always present in the lake.

The results of the present study can be applied in two contexts. First, where the assumptions of local equilibrium with the wind and negligible horizontal transport are valid, the model developed herein is simple enough to be easily integrated into a water-quality model. We expect that parameter values will vary if the model is applied over different sediment types and therefore several sets of parameter calibrations may have to be made for a water-quality model of an entire lake. Second, a more general model of suspended sediment transport, which may include horizontal transport as well as other complicating features, requires the same information on bottom boundary conditions as the present model. Therefore, the results of the present study can be used to specify this boundary condition, although we again expect that different sediment types may require parameter values to be recalibrated.

References

Aalderink, R. H., L. Lijklema, J. Breukelman, W. van Raaphorst, and A. G. Brinkman. 1985. Quantification of wind induced resuspension in a shallow lake. Water Sci. Technol. **17:** 943–954.

Anderson, F. E. 1972. Resuspension of estuarine sediments by small amplitude waves. J. Sediment. Petrol. **42:** 602–607.

Carper, G. L., and R. W. Bachmann. 1984. Wind resuspension of sediments in a prairie lake. Can. J. Fish. Aquat. Sci. **41:** 1763–1767.

CERC. 1974. Shore protection manual. V. 1. U.S. Army Coastal Eng. Res. Center, Ft. Belvoir, Va.

Drake, D. E., and D. A. Cacchione. 1986. Field observations of bed shear stress and sediment resuspension on continental shelves, Alaska and California. Cont. Shelf Res. **6:** 415–429.

Dyer, K. R. 1986. Coastal and estuarine sediment dynamics. Wiley.

Fukuda, M. K., and W. Lick. 1980. The entrainment of cohesive sediments in freshwater. J. Geophys. Res. **85:** 2813–2824.

Gelencsér, P., F. Szilágyi, L. Somlyódy, and L. Lijklema. 1982. A study on the influence of sediment in the phosphorus cycle in Lake Balaton. Int. Inst. Appl. Syst. Anal. Collaborative Pap. CP-82-44.

Grant, W. D., and O. S. Madsen. 1979. Combined wave and current interactions with a rough bottom. J. Geophys. Res. **84:** 1797–1808.

Gross, T. F., A. J. Williams III, and W. D. Grant. 1986. Long-term in situ calculations of kinetic energy and Reynolds stress in a deep sea boundary layer. J. Geophys. Res. **91:** 8461–8469.

Hawley, N. 1983. A numerical model of cohesive suspended sediment dynamics. NOAA Tech. Memo. GLERL-42.

Kamphuis, J. W. 1975. Friction factor under oscillatory waves. J. Waterways Harbors Coastal Eng. Div. (Am. Soc. Civ. Eng.) **101:** 135–144.

Lam, D. C. L., and J.-M. Jacquet. 1976. Computations of physical transport and regeneration of phosphorus in Lake Erie, fall 1970. J. Fish. Res. Bd. Can. **33:** 550–563.

Láng, I. 1986. Impact of policy making: Background to a government decision, p. 110–121. *In* L. Somlyódy and G. van Straten [eds.], Modelling and managing shallow lake eutrophication with application to Lake Balaton. Springer.

Lavelle, J. W., and H. O. Mofjeld. 1987. Do critical stresses for incipient motion and erosion really exist? J. Hydraul. Eng. (Am. Soc. Civ. Eng.) **113:** 370–385.

———, ———, and E. T. Baker. 1984. An in situ erosion rate for fine-grained marine sediment. J. Geophys. Res. **89:** 6543–6552.

Lee, D.-Y., W. Lick, and S. W. Kang. 1981. The entrainment and deposition of fine-grained sediment in Lake Erie. J. Great Lakes Res. **7:** 224–233.

LESHT, B. M., T. L. CLARKE, R. A. YOUNG, D. J. P. SWIFT, AND G. L. FREELAND. 1980. An empirical relationship between the concentration of resuspended sediment and near bottom wave-orbital velocity. Geophys. Res. Lett. **7:** 1049–1052.

LICK, W. 1982. Entrainment, deposition and transport of fine-grained sediments in lakes. Hydrobiologia **91:** 31–40.

———. 1986. Modeling the transport of fine-grained sediments in aquatic systems. Sci. Total Environ. **55:** 219–228.

LIJKLEMA, L., P. GLENCSÉR, F. SZILÁGYI, AND L. SOMLYÓDY. 1986. Sediment and its interaction with water, p. 156–182. *In* L. Somlyódy and G. van Straten [eds.], Modelling and managing shallow lake eutrophication with application to Lake Balaton. Springer.

LUETTICH, R. A., JR. 1987. Sediment resuspension in a shallow lake. D.S. thesis, Mass. Inst. Technol., Cambridge. 311 p.

———, AND D. R. F. HARLEMAN. 1986. A comparison of water quality models and load reduction predictions, p. 323–340. *In* L. Somlyódy and G. van Straten [eds.], Modelling and managing shallow lake eutrophication with application to Lake Balaton. Springer.

———, AND ———. In press. A comparison between measured wave properties and simple wave hindcasting models in shallow water. J. Hydraul. Res.

MCLEAN, S. R. 1985. Theoretical modelling of deep ocean sediment transport. Mar. Geol. **66:** 243–265.

MANTZ, P. A. 1977. Incipient transport of fine grains and flakes by fluids—extended Shields diagram. J. Hydraul. Div. (Am. Soc. Civ. Eng.) **103:** 601–615.

MEHTA, A. J., AND E. PARTHENIADES. 1975. An investigation of the depositional properties of flocculated fine sediments. J. Hydraul. Res. **13:** 361–381.

———, AND ———. 1979. Kaolinite resuspension properties. J. Hydraul. Div. (Am. Soc. Civ. Eng.) **105:** 411–416.

MILLER, M. C., I. N. MCCAVE, AND P. D. KOMAR. 1977. Threshold of sediment motion under unidirectional currents. Sedimentology **24:** 507–527.

MONIN, A. S., AND A. M. YAGLOM. 1971. Statistical fluid mechanics. V. 1. MIT.

OCHI, M. K. 1982. Stochastic analysis and probabilistic prediction of random seas. Adv. Hydrosci. **13:** 217–374.

PARCHURE, T. M., AND A. J. MEHTA. 1985. Erosion of soft cohesive sediment deposits. J. Hydraul. Eng. (Am. Soc. Civ. Eng.) **111:** 1308–1326.

SHANAHAN, P., AND D. R. F. HARLEMAN. 1982. Linked hydrodynamic and biogeochemical models of water quality in shallow lakes. Ralph M. Parsons Lab., Mass. Inst. Technol. Tech. Rep. 268.

SHENG, Y. P., AND W. LICK. 1979. The transport and resuspension of sediments in a shallow lake. J. Geophys. Res. **84:** 1809–1826.

SLEATH, J. F. A. 1984. Sea bed mechanics. Wiley.

SMITH, J. D. 1977. Modelling of sediment transport on continental shelves, p. 539–577. *In* E. D. Goldberg et al. [eds.], The sea. V. 6. Wiley-Interscience.

SOMLYÓDY, L. 1982. Water-quality modelling: A comparison of transport-oriented and ecology-oriented approaches. Ecol. Model. **17:** 183–207.

———, AND G. VAN STRATEN. 1986. Modelling and managing shallow lake eutrophication with application to Lake Balaton. Springer.

SOULSBY, R. L. 1983. The bottom boundary layer of shelf seas, p. 189–266. *In* B. Johns [ed.], Physical oceanography of coastal and shelf seas. Elsevier.

SOUTHARD, J. B., R. A. YOUNG, AND C. D. HOLLISTER. 1971. Experimental erosion of calcareous ooze. J. Geophys. Res. **76:** 5903–5909.

VAN LEUSSEN, W. 1986. Laboratory experiments on the settling velocity of mud flocs, p. 1803–1812. *In* Proc. 3rd Int. Symp. River Sedimentation. Univ. Mississippi.

WILLIAMS, A. J., III. 1985. BASS, an acoustic current meter array for benthic flow-field measurements. Mar. Geol. **66:** 345–355.

WU, J. 1982. Wind-stress coefficients over sea surface from breeze to hurricane. J. Geophys. Res. **87:** 9704–9706.

Submitted: 23 February 1989
Accepted: 21 February 1990
Revised: 30 April 1990

Ecological Modelling, 57 (1991) 173–192
Elsevier Science Publishers B.V., Amsterdam

Influence of sediment resuspension on the light conditions and algal growth in Lake Balaton

L. Somlyódy and L. Koncsos
Water Resources Research Centre VITUKI, Pf. 27, H-1095 Budapest, Hungary
(Accepted 16 January 1991)

ABSTRACT

Somlyódy, L. and Koncsos, L., 1991. Influence of sediment resuspension on the light conditions and algal growth in Lake Balaton. *Ecol. Modelling*, 57: 173–192.

Wind-induced sediment resuspension and its impact on the light conditions were intensively studied in three basins of Lake Balaton, a large shallow lake in Hungary, which is subject to eutrophication. The depth ranges between 2 and 5 m. Frequent observations were made of the wind, the water flows and waves, the suspended solids (ss) concentration, the Secchi disc depth and the light conditions. Four versions of the model were developed for describing the temporal changes in the ss concentration. Models of similar structures were applied for the extinction coefficient and the Secchi disc depth. Several methods were used for calibration. Identifiability and arbitrariness of the model structures have been studied. The extinction model was coupled to a known mass balance equation describing temporal changes in the algal biomass. Sensitivity analysis using hypothetical step-like wind inputs has shown a considerable change in the light limitation factor as compared to the case of steady state winds. Finally, the coupled extinction–algae biomass model was used in a Monte Carlo fashion when longer subsets were selected at random from past wind observations. Late summer conditions and parameters typical for the most eutrophic basin of Lake Balaton (where nutrients are no longer limiting) were selected. The analysis has demonstrated that, in harmony with the observations, the wind has a major impact on the short-term changes of algal biomass. The approach outlined can be utilized to improve the earlier ecosystem models applied for Lake Balaton. The methodology developed is transferable to other shallow lakes.

1. INTRODUCTION

Ecological models are often used for estimating the levels of algal biomass in lakes and evaluating the effectiveness of eutrophication control measures. One of the shortcomings of such models for shallow lakes is that the impact of wind-induced sediment resuspension on the light conditions is not taken into account. This issue is addressed here on the basis of

0304-3800/91/$03.50

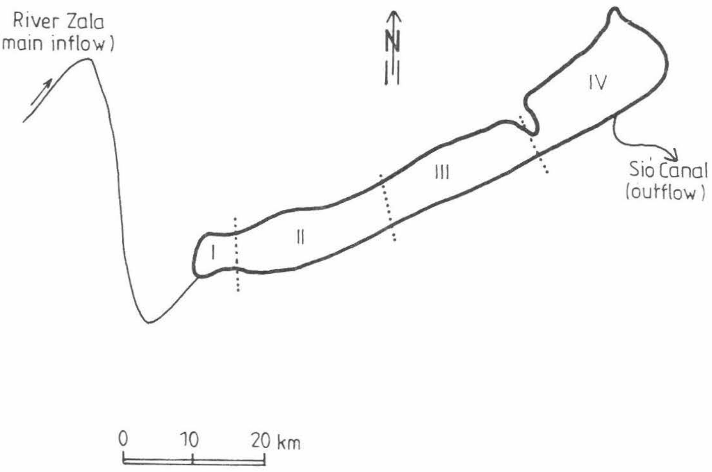

Fig. 1. Lake Balaton. I, Keszthely basin; II, Szigliget basin; III, Szemes basin; IV, Siófok basin.

experiences gained in relation to Lake Balaton in Hungary. Lake Balaton (Fig. 1) is the largest shallow lake in Europe, a typical wind-affected water body. This lake of elongated shape consists of four segments of different characters known, from west to east, as the Keszthely, Szigliget, Szemes and Siófok basins (Somlyódy and van Straten, 1986). The prevailing wind direction is approximately perpendicular to the longitudinal axis of the lake, leading to effective mixing in the cross sections and determining the fetch conditions.

The manmade eutrophication of the lake has been studied intensively during the past fifteen years and in 1983 a comprehensive phosphorus abatement program was launched. For details we refer the reader to Somlyódy and van Straten (1986). Here, it suffices to mention that the specific phosphorus load is about ten times higher in the westernmost basin of the lake than in Siófok bay and consequently the trophic state also varies longitudinally from hypertrophic to eutrophic at Keszthely to mesotrophic at Siófok (Fig. 1).

Wind-induced resuspension and its impact on the light conditions have been systematically analysed during the past ten years in three basins, where the depths range between 2 and 5 m, and wind speed fluctuates between 0 and 15 m s^{-1}. For details the reader is referred to Somlyódy (1986), Luettich et al. (1990) and Section 2.3, which offers a brief summary of the evaluation of the model parameters from the experiments, and a discussion of the identifiability of the model structure.

Algal growth as a function of the temporally strongly variable light conditions (owing to the action of the wind) was not studied experimentally: in this respect we apply algal models taken from the literature (see later). In specific terms this means that we accepted the validity of Steele's equation for light limitation (Steele, 1962) (although this equation is not considered to be fully adequate for all conditions occurring in nature, Straškraba, 1976). In addition, no adaptation of algae to changes in light conditions within a day was assumed that is in harmony with the derivation of Steele's equation and present modelling practices. If fast adaptation takes place, the impact of sediment resuspension on algal dynamics will be smaller than that to be presented here.

2. GOVERNING EQUATIONS

2.1. Conventional approach

Algal dynamics in a lake is most commonly described (see, e.g., Orlob, 1983; Thomann and Mueller, 1987; Somlyódy and van Straten, 1986) by the equation:

$$\mathrm{d}A/\mathrm{d}t = k_{\mathrm{g}} f_{\mathrm{T}} f_{\mathrm{P}} f_{\mathrm{N}} f_{\mathrm{I}} A - k_{\mathrm{d}} \Theta^{(T-T_0)} A \tag{1}$$

expressing the day-to-day changes in algal biomass A (averaged over depth, H) as a consequence of the difference between growth and mortality rates (disregarding inflows, outflows and sedimentation). In equation (1), k_{g} is the specific maximum growth rate coefficient, f_{T} is the temperature reduction factor, f_{P} and f_{N} are the phosphorus (P) and nitrogen (N) limitation factors, f_{I} is the light limitation (or attenuation) factor, k_{d} is the mortality rate coefficient at temperature T_0, Θ is the mortality temperature coefficient, T is the actual temperature and t is the time. The temperature and nutrient limitation factors can be specified as follows:

$$f_{\mathrm{T}} = \begin{cases} \dfrac{T_{\mathrm{c}} - T}{T_{\mathrm{c}} - T_0} \exp\left(1 - \dfrac{T_{\mathrm{c}} - T}{T_{\mathrm{c}} - T_0}\right) & \text{if } T \leqslant T_{\mathrm{c}} \\ 0 & \text{if } T > T_{\mathrm{c}} \end{cases} \tag{2}$$

$$f_{\mathrm{P}} = \frac{P}{P_{\mathrm{k}} + P} \quad \text{and} \quad f_{\mathrm{N}} = \frac{N}{N_{\mathrm{k}} + N} \tag{3}$$

where T_{c} is the critical temperature, P and N are dissolved inorganic nutrient concentrations, and P_{k} and N_{k} are half-saturation constants.

The light attenuation factor is derived with Steele's equation (see, e.g., van Straten, 1980; Straškraba and Gnauck, 1985; Thomann and Mueller, 1987):

$$f(I) = \frac{I}{I_{\mathrm{s}}} \exp\left(1 - \frac{I}{I_{\mathrm{s}}}\right) \tag{4}$$

incorporating the influence of light inhibition on algal growth at light intensities (I) larger than the saturation or optimal value (I_s). Furthermore, assuming the validity of the Lambert–Beer law for the vertical penetration of light in water (which has been confirmed for Lake Balaton, see Koncsos, 1990):

$$I(z) = I(0)\exp(-\epsilon z) \tag{5}$$

where z is the vertical coordinate measured downwards from the free surface, $z = 0$, and ϵ is the extinction coefficient (m^{-1}), the depth-integrated form of the light limitation factor is:

$$\bar{f}(I) = \frac{1}{H}\int_0^H f(I)\,\mathrm{d}z = \frac{e}{\epsilon H}\left[\exp\left(-\frac{I(H)}{I_s}\right) - \exp\left(-\frac{I(0)}{I_s}\right)\right] \tag{6}$$

Here $I(H)$ is the light intensity at the bottom of the lake.

Since equation (1) refers to the daily variation of algal biomass, for final use we require $\bar{\bar{f}}(I)$, the day averaged form of the light limitation factor $\bar{f}(I)$. An analytical integration is possible if certain idealized diurnal light patterns are used as approximations. For instance, for triangular light patterns we obtain (see van Straten, 1980):

$$\begin{aligned} f_1 &= \bar{\bar{f}}(I) \\ &= \frac{e\lambda}{\epsilon H}\left(\frac{1}{2L(H)}\{1 - \exp[-2L(H)]\} - \frac{1}{2L(0)}\{1 - \exp[-2L(0)]\}\right) \end{aligned} \tag{7}$$

where

$$L(0) = R/\lambda I_s \tag{8}$$

$$L(H) = L(0)\exp(-\epsilon H) \tag{9}$$

Here R is the daily total of global radiation and λ is the length of the photoperiod (–). Equation (7) is highly non-linear and quite sensitive to the value of the extinction coefficient, particularly if ϵH is below five (the case of transparent shallow water, see van Straten, 1980).

Equation (7) is widely used in the literature with the assumptions that the extinction coefficient is determined by the colour of water without algae and the self-shading effect is expressed by the coefficient α as follows

$$\epsilon = \epsilon_0 + \alpha A \tag{10}$$

Unfortunately, in shallow lakes extinction is strongly influenced by the concentration of suspended solids (ss),

$$\epsilon = \epsilon_0 + \alpha A + \epsilon_{ss} \tag{11}$$

where ϵ_{ss} is assumed to be linearly related to the concentration of ss:

$$\epsilon = \epsilon_0 + \alpha A + \beta\,\mathrm{ss} \tag{12}$$

Since the concentration of ss fluctuates on a much shorter time scale than the algal biomass because of the wind-induced sediment resuspension, equation (7) may lose its validity and for this reason a numerical integration of equation (6) is required (after introducing equation (11)).

In a different formulation, two questions should be raised for shallow-water bodies:

(1) the role of the wind-dependent component of the extinction coefficient (the order of magnitude of which can be characterized by its daily average);

(2) the importance of the temporal change of ϵ_{ss} on a time scale of days.

2.2. Approach to dynamic models for suspended solids and extinction coefficient

To describe temporal changes of the ss concentration averaged for particular 'uniforms' segments of Lake Balaton, a sequence of simple mass balance models was developed in the following form:

$$H \, \mathrm{dss}/\mathrm{d}t = \phi \tag{13}$$

where ϕ is the residual, vertical flux of sediment at the bottom of the lake, which is assumed to be the sum of the impact of deposition (ϕ_d) and resuspension (ϕ_e):

$$\phi = \phi_d + \phi_e \tag{14}$$

Equation (13) implies that temporal changes in the concentration of suspended solids are primarily the result of vertical transport and that the contribution of horizontal convection and turbulent diffusion can be disregarded. The validity of this assumption could be justified for Lake Balaton on the basis of an analysis of the scales of time and length of the three-dimensional mass flow equation of suspended sediment as was done by Luettich et al. (1990). Similar conclusions were drawn by Koncsos (1990) who compared the completely mixed reactor model, equation (13), to a corresponding longitudinal dispersion equation for the shallowest, westernmost basin of Lake Balaton. For convection and dispersion, the actual simulation results derived by Shanahan et al. (1986) from a two-dimensional hydrodynamic model were utilized and longitudinal changes in the ss concentration typical for Lake Balaton were assumed. The analysis has shown practically no deviations between the two approaches for stormy conditions. The largest difference was obtained for periods subsequent to larger storms when resuspension had already ceased to act but longitudinal seiche motion was still significant. This difference, however, could be considered as small too and therefore the assumption of complete mixing for a lake segment was accepted.

In all the model versions ϕ_d was considered to be proportional to the average depth concentration minus the background value (ss_0) (expressing the presence of very fine material mostly of organic origin, which is in suspension at all times):

$$\phi_d = k_1(ss - ss_0) \tag{15}$$

where k_1 is the apparent settling velocity.

For ϕ_e several hypotheses were tested. First, the assumption that:

$$\phi_e = k_2 W^n \tag{16}$$

was made (Somlyódy, 1982, 1986) in which the positive constants k_2 and n_1 together with k_1 and ss_0 were estimated from *in situ* time series types of observations of ss and the wind speed W (see later). This model has been succesfully applied to Lake Veluwe, a shallow water body in the Netherlands (Aalderink et al., 1985).

A refinement of the resuspension term was derived by Luettich et al. (1990):

$$\phi_e = k_3(\tau - \tau_{cr})^{n_1} \tag{17}$$

where τ is the wave-induced bottom shear stress, which can be derived from linear wave theory, τ_{cr} is the critical shear to be estimated from observations together with the model parameters k_3 and n_1. As shown by Luettich et al. (1990), equation (17) can be replaced (for a laminar boundary layer, which is the case for Lake Balaton) by:

$$\phi_e = k_4(H - H_{cr})^{n_2} \tag{18}$$

where H is the significant wave height, and H_{cr} is its critical value; H can be derived from the Sverdrup–Munk–Bretschneider shallow-wave 'hindcasting' (predication) method (CERC, 1977), and k_4 and n_2 are constants as before. The model obtained was calibrated and validated on the basis of detailed observations performed in August 1985 in the Keszthely basin of Lake Balaton. For details, the reader is referred to Luettich et al. (1990).

Equations (17) and (18) are physically better supported than equation (16) and their application has slightly decreased deviations between computations and observations. However, the improvement was relatively insignificant because of the similarity $H(t) \sim W(t)$ found for the situations analysed.

Finally, Koncsos (1990) introduced two sediment fractions (but maintained equation (16)) and improved the model behaviour primarily for moderate wind conditions and periods after major storms for which the earlier model versions resulted in faster declines in the ss concentration than the observations.

Summarizing the experiences gained with the versions of the model outlined here, it can be stated that although a step-by-step improvement was achieved, the differences in performances between the alternative models are still small. For this reason, we use the simplest version of the model for our present objectives.

According to equation (12) the suspended solids concentration and the extinction coefficient are linearly related. From this assumption it follows that a model similar to equations (13)–(16) should also be valid for the ss-dependent component:

$$H\frac{\mathrm{d}\epsilon_{ss}}{\mathrm{d}t} = -k_1^*\epsilon_{ss} + k_2^*W^{n^*} \tag{19}$$

where k_1^*, k_2^* and n^* are again positive model parameters.

The extinction model introduced results in considerable hourly changes in ϵ_{ss} depending on the prevailing wind conditions. The total extinction coefficient (see equation (12)) can be used subsequently as the input for obtaining the daily average light attenuation factor from the numerical integration of equation (6). The systematic application of this procedure allows us to judge the importance of the sediment resuspension on the light limitation factor and, by the application of equation (1), on the daily algal dynamics.

2.3. Estimating the parameters of the models for ss *and* ϵ_{ss}

Three sequences of the measurement periods have been utilized for estimating the model parameters.

(1) Daily observations of ss and Secchi disc depth (Z_S) in the middle of Szemes basin (Fig. 1, $H = 4.3$ m) for five months in 1979 (hourly wind data were available).

(2) Bi-weekly observations of the extinction coefficient made in 1977 (Herodek et al., 1982) in the easternmost basin at Siófok ($H = 5.0$ m), for which hourly wind data were collected for the entire year.

(3) Results of a two-week experimental program when, among others, the wind speed and direction, the water velocity, the characteristics of wave motion, ss, Z_S and the light conditions were recorded in the Keszthely basin (Fig. 1, $H = 2.0$ m) (see Luettich et al., 1990). Several parameters (e.g., wind data, water velocity) were monitored nearly continuously. The sampling frequencies of the suspended solids concentrations ranged between 10 minutes and 2 hours.

For parameter estimation several methods such as the extended Kalman filter (EKF), the Marquardt algorithm, and a new global optimization procedure have been applied. Details can be found in Somlyódy (1986) and Luettich et al. (1990). Here, only a brief summary is given.

No unique combination of parameters was found to be 'optimal'. Rather a certain range of approximately equal root mean square errors resulted. On the basis of a detailed analysis Luettich et al. (1990) found that k_1 was the only parameter that was not correlated with the others. This key parameter, the sedimentation velocity, can be determined in principle by independent experiments.

The above behaviour raises the issue of model structure identification (see, e.g., Beck, 1979), arbitrariness and modelling poorly defined systems (see, e.g., Fedra et al., 1981) in relation to which we have the following comments:

(1) The time invariability of the parameters has been demonstrated by the application of the EKF method (Somlyódy, 1982).

(2) All the model versions (hypotheses) tested have shown similar features from the viewpoint of identifiability.

(3) This fact is not a consequence of uncertainties in the data and forcing functions but rather that of the strong coupling between two processes, that is sedimentation and resuspension, the balance of which defines relatively well the equilibrium concentration:

$$ss_e = (k_2/k_1)W^n \tag{20}$$

belonging to a given wind speed (here $ss_0 = 0$ was assumed). This coupling is characterized by $k_2/k_1 = \text{const}$ if the exponent is fixed.

(4) Similar features can be observed, for example, also for depth-integrated hydrodynamic models of lakes where the drag coefficient and the friction coefficient (characterizing shear stresses at the surface and bottom, respectively) compensate each other in a certain domain (Somlyódy, 1983). If they could be measured directly and accurately, the model would be sound and well defined. Since this is not the case (the parameters are aggregated in character) the model structure cannot be identified from the point of view of systems theory and several combinations of the two coefficients result in practically the same model performance (Somlyódy, 1983).

Returning to our present problem, the situation is the same: approximation of sophisticated physical processes, aggregating, the presence of compensating processes and the lack of direct determination of most of the parameters lead to a lack of identifiability.

Returning to the parameter values, $ss_0 = 0$–15 g m^{-3}, $n = 1$, and $k_2/k_1 = 6$–7×10^{-2} kg m^{-4} were found to be satisfactorily for all the experiments.

The value of k_1 was the same for the Szemes and Siófok basins ($k_1 = 6.5 \times 10^{-5}$ m s^{-1} corresponding to 5.5 m d^{-1}) in harmony with the properties of the sediments. However, the situation is different for the Keszthely basin: here the estimated settling velocity of ss is about 3–4 times higher than at Siófok or Szemes, although the bottom sediment is finer.

The explanation of this seeming contradiction is that during storms coarse sediment fractions are also stirred up at Keszthely (where the water depth is less) which then settle faster when the wind declines. The presence of this phenomenon was fully confirmed by the two-fraction model of Koncsos (also see later).

As far as the parameters of the extinction model are concerned, $k_1^* = k_1$ and $n^* = n$, while k_2^* is about one tenth that of the ss model (corresponding to the results of a regression analysis with equation (12) leading to a value close to 0.1). The reasonable behaviour of the model is illustrated in Fig. 2, which compares the observed and simulated results for the Siófok basin (Herodek et al., 1982).

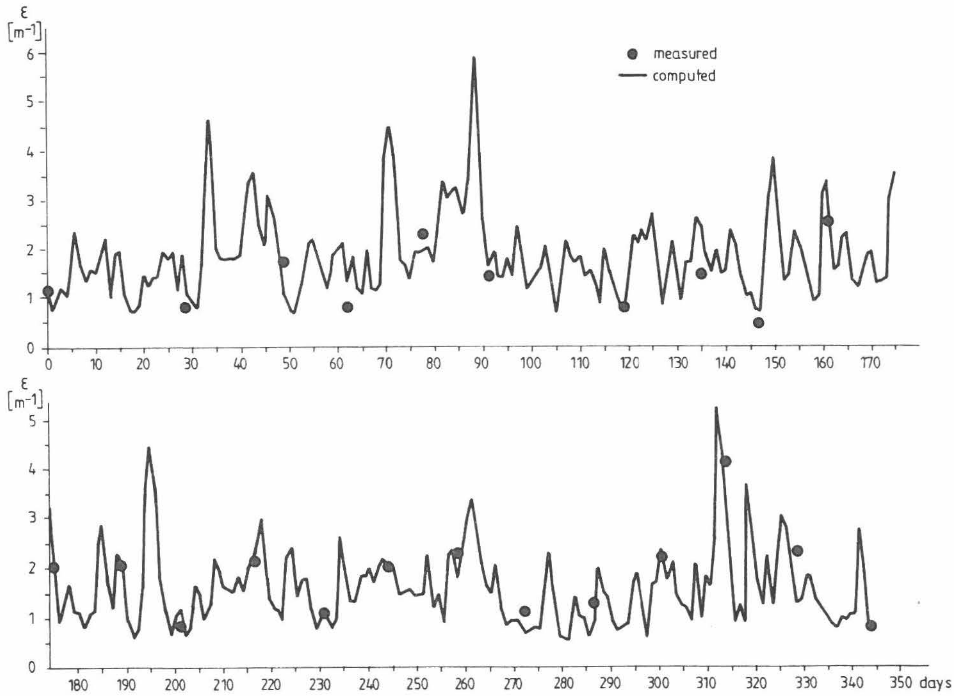

Fig. 2. Validation of the extinction model (Siófok basin, Lake Balaton, 1977).

In summary, the following parameters have been obtained for equation (19):

$k_1^* = 6.5 \times 10^{-5}$ m s^{-1} $\quad$ $k_2^* = 4.5 \times 10^{-6}$ m^{-1}

for the Szemes and Siófok basins, respectively, and:

$k_1^* = 28.0 \times 10^{-5}$ m s^{-1} $\quad$ $k_2^* = 29.0 \times 10^{-6}$ m^{-1}

for the Keszthely region (and $n^* = 1$ for all the cases). The latter parameter set will be utilized for further analysis. It is noted that the steady-state solution of equation (19) is similar to (20) leading to an equilibrium extinction coefficient $\epsilon_{SSe} = 0.7$–1.0 W m^{-1} with the above parameters.

3. RESULTS

We perform three types of analyses. First, idealized, step-like, deterministic wind inputs are used for evaluating the possible influence of dynamic

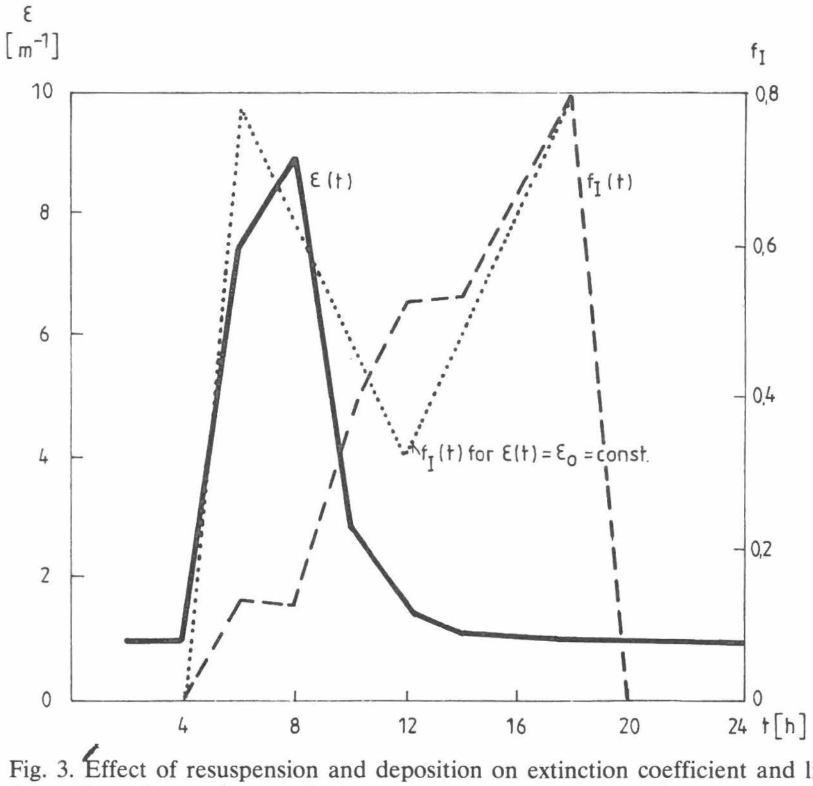

Fig. 3. Effect of resuspension and deposition on extinction coefficient and light limitation factor ($W = 12$ m s^{-1}, $t_0 = 4h$, $\Delta t = 6$ h, $\epsilon_0 H = 2.5$, $R/\lambda I_s = 7$).

resuspension events on the light limitation factors. Second, the same exercise is performed by selecting at random daily 'windows' from observed past wind records. Finally, longer subsets of the same data series are chosen, also in a Monte Carlo fashion, for computing the impact on algal dynamics as compared to the conventional approach.

3.1. Sensitivity of the light limitation factor for step-like wind inputs

Equations (19), (11) and (6) are solved for step-like wind inputs: a wind of constant speed W starts to blow at a time t_0 for a duration of Δt. As can be seen from Fig. 3, ϵ increases significantly owing to resuspension within a short period of time, while after the decay of the hypothetical storm it declines exponentially as defined by sedimentation. The light limitation factor changes simultaneously between 0 and 0.8 as determined by the dynamics of extinction and the coincidence of the storm and the photoperiod (the parameter $R/\lambda I_s$ was selected as typical for summer conditions at Lake Balaton). Its pattern differs significantly from the $\epsilon(t) = \epsilon_c$ = constant case (Fig. 3).

In order to evaluate the non-linear influence of wind on the daily average light limitation factor, the parameters W, t_0 and Δt were systematically changed. The results for $W = 12$ m s^{-1} are given in Fig. 4 as a function of t_0. When there is no wind, f_I is about 0.3 for the parameters

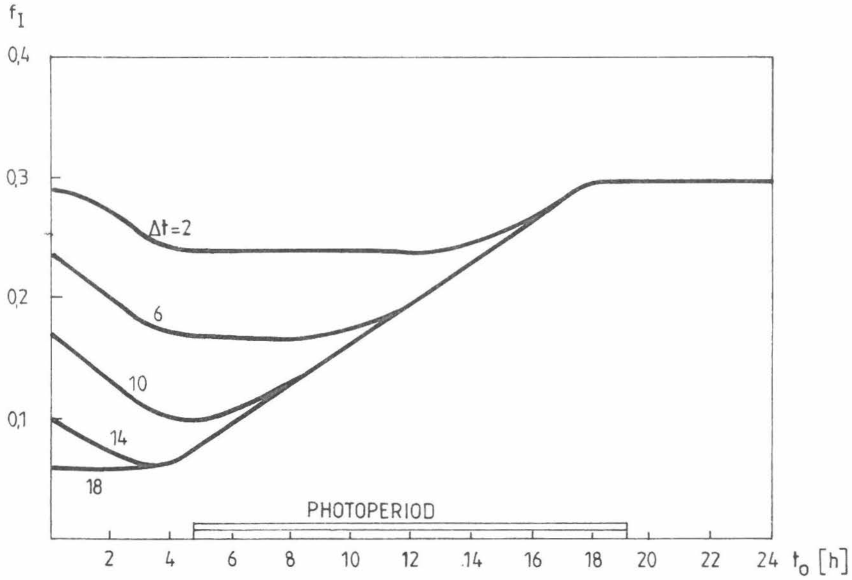

Fig. 4. Change of light limitation factor (as a function of wind parameters for step-like input) ($W = 12$ m s^{-1}, $\epsilon_0 H = 5$, $R/\lambda I_s = 7$).

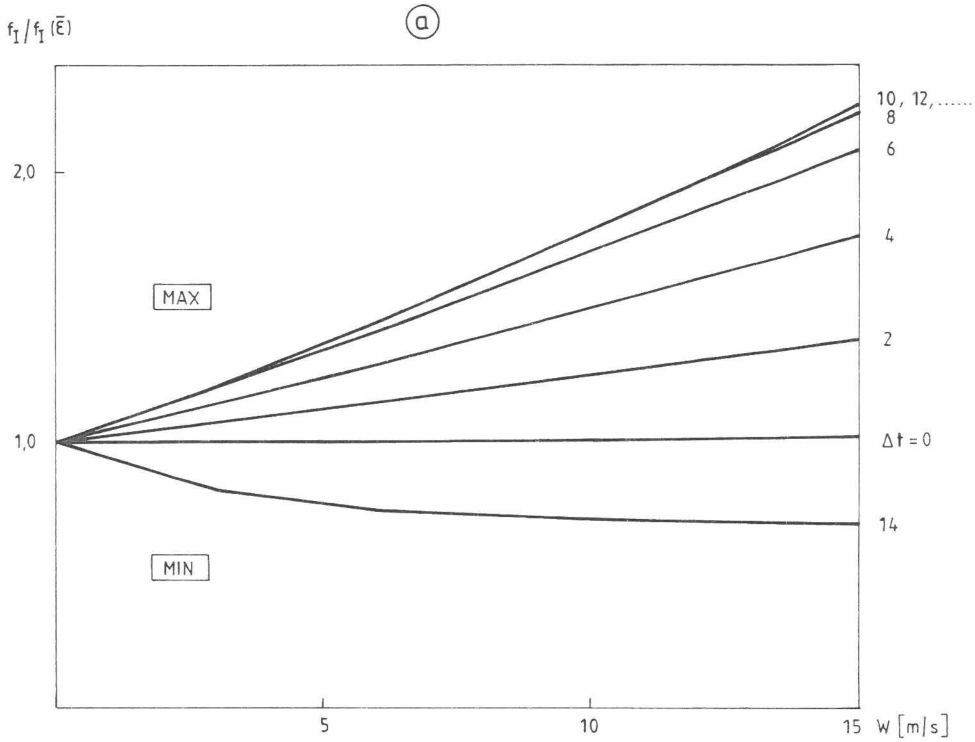

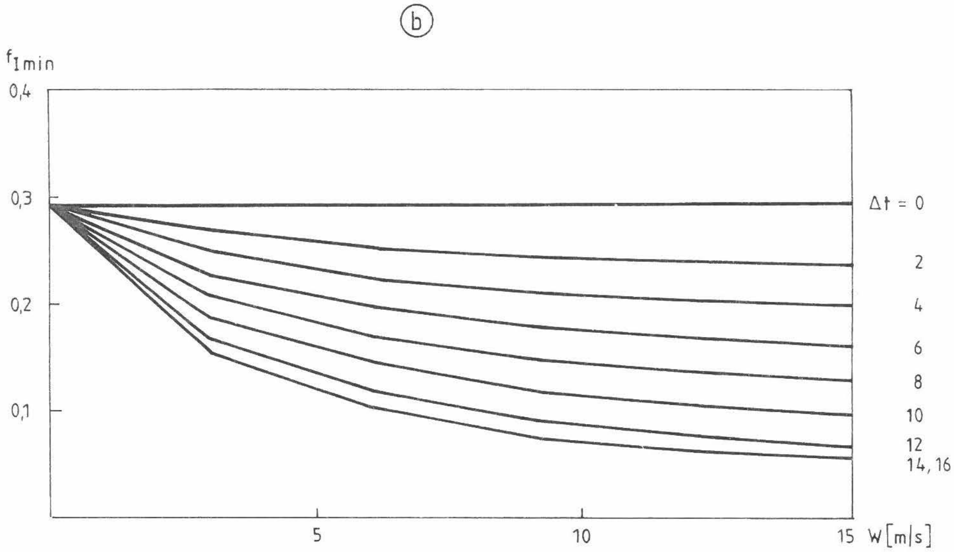

Fig. 5. Daily extremes of light limitation factor ($\epsilon_0 H = 5$, $R/\lambda I_s = 7$).

assumed and then decreases to about 0.05 as the photoperiod and the duration of the storm increasingly overlap.

From Fig. 4 the smallest and largest values of f_I can be selected and plotted against wind speed, considering t as a parameter. One such summary is given in Fig. 5. Figure 5a illustrates the changes in the extremes related to the light limitation factor obtained by using $\bar{\epsilon}$, the daily average of the temporally variable extinction coefficient $f_I/f_I(\bar{\epsilon})$ (see Fig. 3). The approximately linear influence of W and the saturation character as a function of duration are the two main conclusions to be drawn from the figure. Figure 5b shows the variation of $(f_I)_{min}$. The saturation type of behaviour can also be observed here, but the impact of wind speed is basically non-linear in nature.

3.2. Real wind events and the light limitation factor

The wind record of the 1979 observations mentioned above was used for the random selection of 24-hour windows. For each event the same evaluation was made as outlined in section 3.1. Depth, background extinction coefficient values and model parameters were taken as characteristic for the Keszthely basin. Light limitation factors obtained were plotted against daily average wind speed. The results of 200 simulations are presented in Fig. 6.

It can be seen that f_I shows a hyperbolic decrease with wind speed from about 0.19 to 0.07 and the scatter depending on wind history is considerable (around +/− 20%). The exclusion of wind influence leads to a significant error in the light attenuation factor.

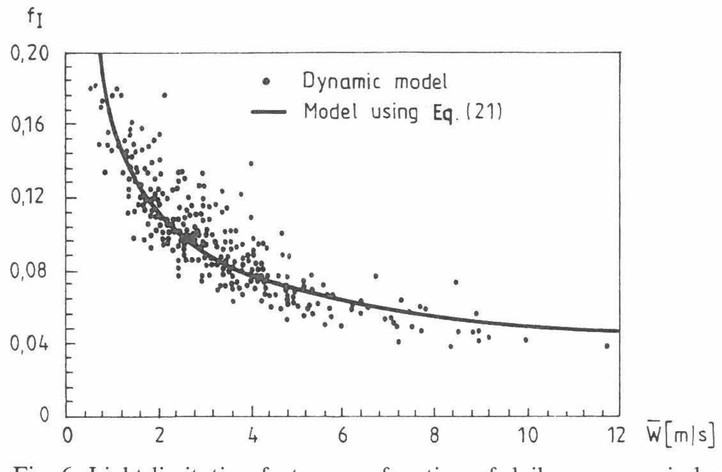

Fig. 6. Light limitation factor as a function of daily average wind speed (200 Monte Carlo simulations).

Comparing the daily average light limitation factor of this procedure to that gained from equation (7) by using the daily mean value of the extinction coefficient ($\bar{\epsilon}$), an approximately one-to-one relation is obtained with a relative standard deviation of about 10% (the correlation coefficient is 0.84).

However, $\bar{\epsilon}$ is unknown, a difficulty that can be resolved by employing the steady-state solution of equation (19) for ϵ_{ss} (see equation (12)):

$$\bar{\epsilon} = \epsilon_0 + \alpha A + \beta^* \overline{W} \tag{21}$$

As shown by Fig. 6 such an approach improves the situation as the mean variation is captured quite well. This still leaves the problem that the parameter β^* has to be determined on the basis of the dynamical model (as has been done here) or estimated together with all the other parameters of the ecosystem model selected. We note that the value $\beta^* = 1.3$ obtained is slightly higher than the one found in Section 2.3.

3.3. Impact on algal biomass

At this stage of the study 14-day subsets are selected at random (with replacement) from the same wind record as before and equations (1), (2), (3), (6), (11) and (19) are solved in a Monte Carlo fashion. Parameters representative of the Keszthely basin are used again. On the basis of the experiments performed, $\epsilon_0 = 2$ m^{-1} and $\alpha = 0.019$ m^2 mg^{-1} were selected for background extinction and self-shading coefficients. As external factors are concerned, the constant temperature and solar radiation typical for August were considered ($T = 20\,^\circ$C and $R/\lambda I_s = 7$ were selected). Because of the high internal phosphorus load and the dominance of blue–green algae (see Somlyódy and van Straten, 1986) nutrients were considered as not limiting growth ($f_P = f_N = 1$). Other parameters were chosen on the basis of recent experiences related to modelling the behaviour of the ecosystem of the Keszthely basin (e.g., $k_g = 7.2$ d^{-1}, $k_d = 1.8$ d^{-1}, see also Somlyódy and van Straten, 1986).

Figure 7 shows the increase in algal biomass (expressed in chlorophyll-*a*) from an initial value of $A(0) = 30$ mg m^{-3}. In addition to the expected values, the standard deviations and extreme values are also given (from 200 simulations).

4. DISCUSSION

4.1. Discussion of the results of Section 3

As a starting point we use Fig. 7 on the basis of which several comments can be made:

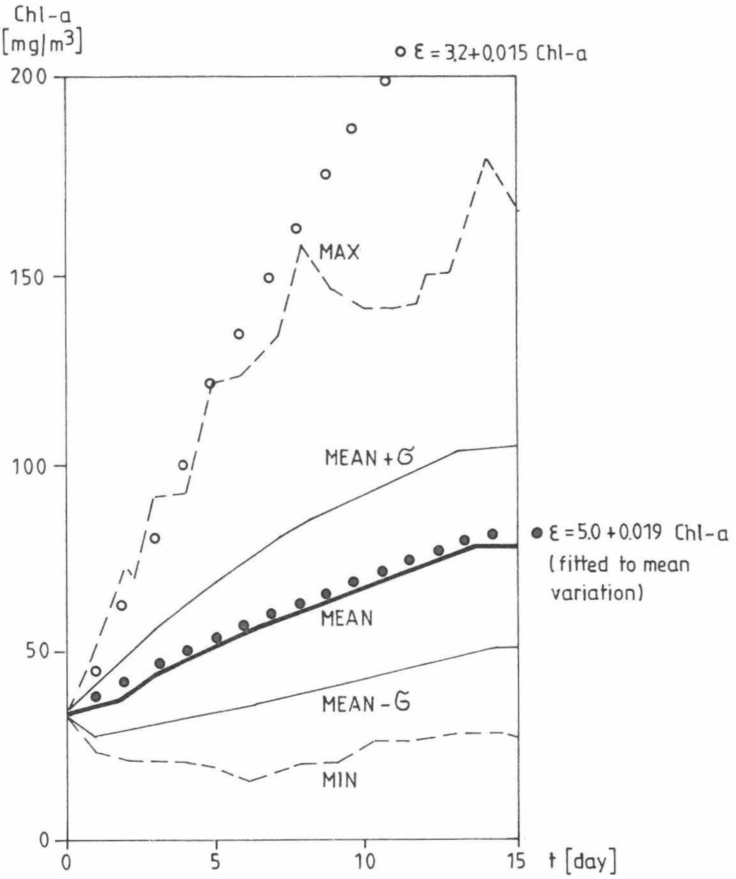

Fig. 7. Wind impact on algal biomass: Monte Carlo simulations for the Keszthely basin.

(1) The expected values show a continuous increase up to about 75 mg m^{-3}, which can be considered as a moderate algal level in late summer at the westernmost part of Lake Balaton. The standard deviation exceeds 30%, while the maximum values are close to 200 mg m^{-3} as is frequently observed nowadays.

(2) In contrast to the smooth variation of the statistical parameters of Fig. 7, individual simulations show a much more 'chaotic' behaviour. A short period (of a few days) with little wind combined with a low extinction coefficient can lead to a biomass of above 150 mg m^{-3}, which then collapses just as quickly as the wind and turbidity increase (self-shading plays a role, too). Figure 8 demonstrates clearly the composition of the extinction coefficient and the influence of two moderate storms in ending algal growth.

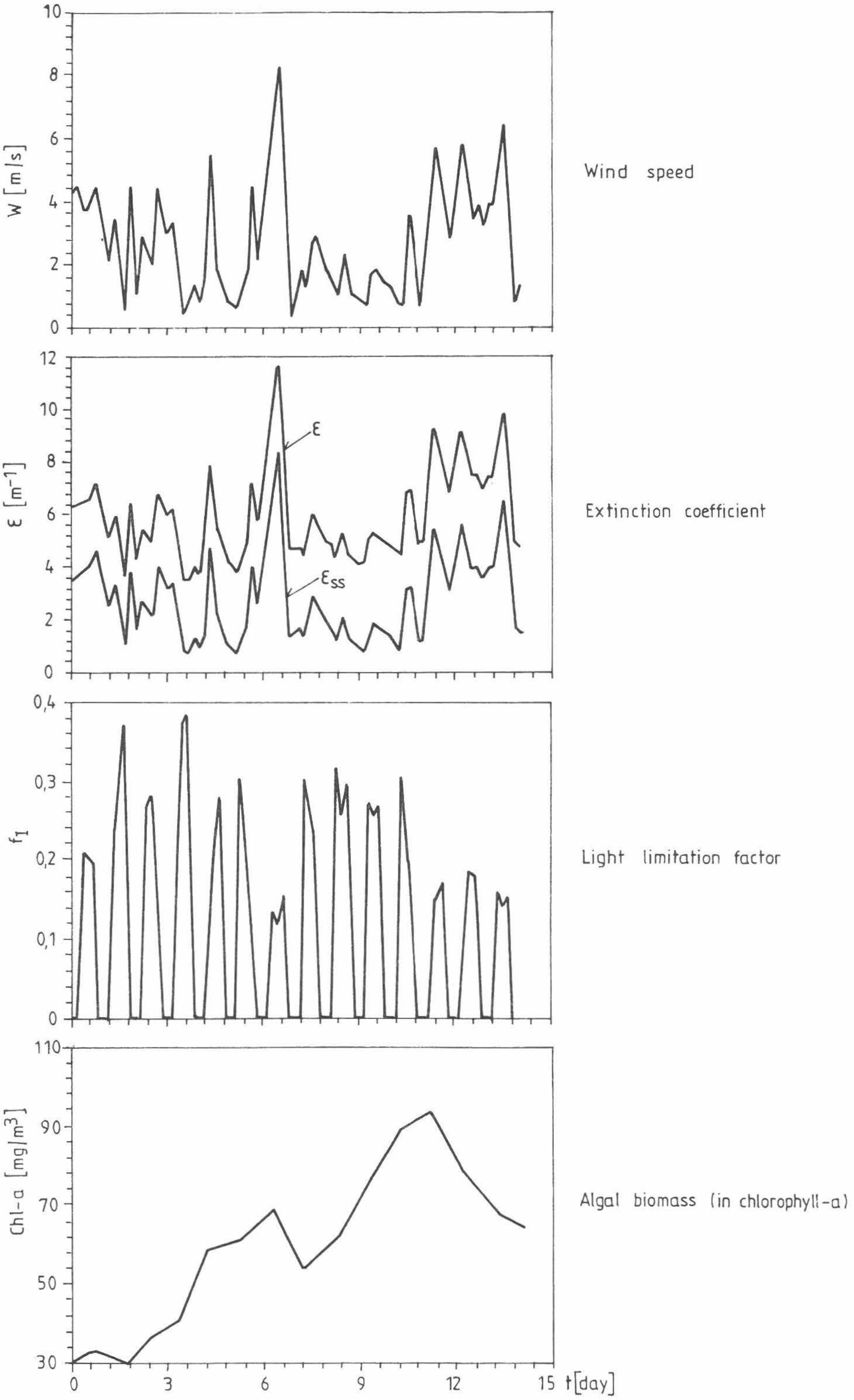

W [m/s]
Wind speed
ε [m⁻¹]
ε
ε_ss
Extinction coefficient
f_I
Light limitation factor
Chl-a [mg/m³]
Algal biomass (in chlorophyll-a)
t[day]

The above phenomenon is frequently observed in the western segments of Lake Balaton in late summer: the wind (and other meteorological factors) causes a considerable degree of randomness in the algal biomass, which earlier phytoplankton models that excluded wind were unable to capture.

(3) Failure to take the impact of the wind into account can lead to a considerable error in predicting short-term changes in biomass [see item (5) later]. Use of equation (21) with the daily average wind speed leads to practically the same mean variation as presented in Fig. 7 but the standard deviations and peak values are slightly higher. The explanation of this surprising behaviour is the overestimate in f_I for small wind speeds as is suspected from Fig. 6.

Judging the applicability of equation (21) for predictions requires the comparison of individual simulations with those obtained from a more detailed model (see Fig. 9 for two runs for a four-week period, one characterized by good agreement, the other by considerable differences). One possible way is to calculate the daily deviations (d_i) between the two solutions for all wind scenarios (j) of the Monte Carlo procedure and then to perform a statistical evaluation. Such an analysis shows that the bias, $E[E_j(d_i)]$ is 12 mg m^{-3} (about 25% of the 'mean' biomass), while the standard deviation of the above estimate is 17 mg m^{-3}. Corresponding values for the standard deviation $\sigma_i(d_i)$ are 13 mg m^{-3} and 6 mg m^{-3}. All these characteristics show that in spite of the acceptable agreement in mean variations of Monte Carlo simulations for the two approaches, the temporal patterns of individual solutions can differ considerably and deviations can reach 40–50 mg m^{-3} (see Fig. 9). The relatively high bias found is explained by the cumulative character of the errors: deviations belonging to a particular day are generally maintained for the rest of the period (as shown by scenario (1) of Fig. 9).

(4) Section 3.1 has led to a relatively large sensitivity of f_I to short-term changes of wind, assuming a hypothetical step-like pattern. Present experience shows that in the absence of sudden changes in the real wind record used this influence is smaller and effective primarily for conditions when ϵ and H (and thus ϵH) are small (see also section 2.1).

(5) If the wind is completely excluded, two model parameters related to light are available to fit simulations to observations, namely ϵ_0 and α. Parameters used in earlier Lake Balaton ecosystem models assuming P limitation (Somlyódy and van Straten, 1986) would lead to an overprediction in biomass under the present conditions ($f_P = f_N = 1$, see Fig. 7). An

Fig. 8. Step-by-step illustration of wind influence on algal biomass.

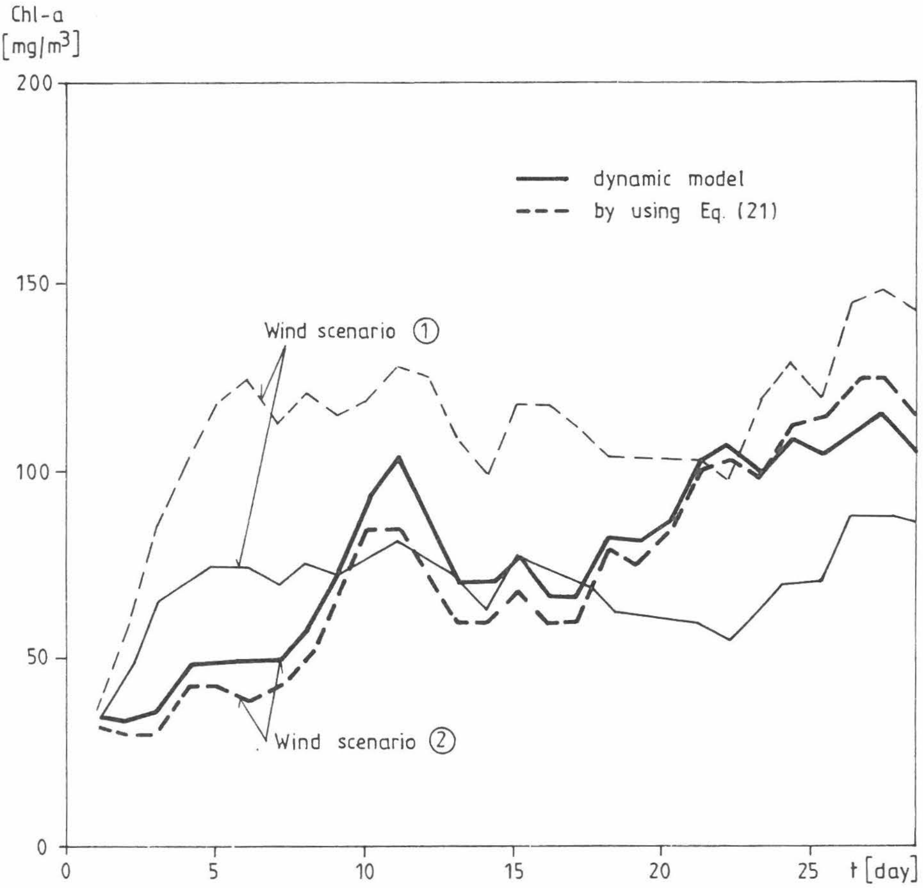

Fig. 9. Comparison of the solution obtained by using equation (12) to that of the dynamic model for two wind scenarios.

acceptable matching could be obtained by increasing ϵ_0 to 5 m^{-1}, which, however, is an unrealistically high value.

As compared to the above, illustrative example, disregard of ϵ_{ss} causes an increasing error if the algal biomass or water depth is smaller, but conditions are favourable for growth. In contrast, nutrient limitation, high biomass, depth and background extinction will reduce the influence of sediment resuspension.

4.2. Outlook for conditions differing from those of Lake Balaton

Lake Balaton has many specific features from the point of view of the present subject, such as its shape, depth and fetch conditions, wind characteristics, wave patterns, sediment composition and particle size distributions, phytoplankton structure and others. All these mean that although wind-induced sediment resuspension and its impact on the light conditions are probably of similar importance for many other shallow lakes, the quantification requires site-specific observations and research in each particular case. This is especially true for the composition of sediment. If, for instance, we consider the experiences gained for Lake Veluwe (Aalderink et al., 1985), we find that although the ss model outlined here proved to be the most acceptable among the versions tested, the parameters were quite different. The background concentration was higher and the temporal changes of suspended solids concentration were smaller than for Lake Balaton, presumably because of the higher organic material content of the sediment.

Even the experiences gained for the Keszthely basin indicate the importance of the dependence between the strength of shear acting at the bottom and the particle size distribution of sediment stirred up: the two-fraction model calibrated for a period of two major storms has shown the dominance of two drastically differing sediment fractions with sedimentation velocities of 2 m d^{-1} and 100 m d^{-1}, respectively (Koncsos, 1990).

The Sverdrup–Munk–Bretschneider shallow-wave 'hindcasting' method can provide useful experience for the study of the influence of variable water depth on resuspension under unchanged sediment composition. For instance, it was found that for the fetch conditions of Lake Balaton, the bottom shear stress increases strongly as the water depth decreases below 3 m. For $W = 15$ m s^{-1} and $H = 3$ m the bottom shear is about an order of magnitude smaller than for $H = 1$ m (and roughly equals the value obtained for the latter depth at half speed). This behaviour explains why the parameters were found to be similar for the two eastern basins of Lake Balaton but differing from that of the much shallower westernmost basin.

In summary it can be said that the methodology presented here can be successfully applied to other shallow lakes, too. Model equations are simple and can be easily incorporated into ecological models. They can be employed jointly with a shallow-wave hindcasting method for planning purposes (e.g., the design of an artificial lake in which a certain ss level needs to be maintained to limit eutrophication).

Several fields can be identified for future research, including the connection between unsteady bottom shear stress and resuspension of sediment of various compositions and the dependence of algal growth on temporally strongly variable light conditions.

REFERENCES

Aalderink, R.H., Lijklema, L., Brenkelman, J., van Raaphorst, W. and Brinkman, A.G., 1985. Quantification of wind induced resuspension in a shallow lake. Water Sci. Technol., 17: 943–954.

Beck, M.B., 1979. Model structure identification from experimental data. In: E. Halfon (Editor) Theoretical Systems Ecology. Academic Press, New York, pp. 259–239.

CERC, 1977. Shore Protection Manual. Vol. 1. U.S. Army Coastal Engineering Research Center, Fort Belvoir, VA.

Fedra, K., Van Straten, G. and Beck, M.B., 1981. Uncertainty and arbitrariness in ecosystems modelling: a lake modelling example. Ecol. Modelling, 13: 87–110.

Herodek, S., Vörös, L. and Tóth, F., 1982 Phytoplankton mass and the eutrophication of Balaton. The Szemes Basin (1976–77) and Siófok Basin (1977). Hidrológiai Közlöny, 62: 220–229 (in Hungarian with English Summary).

Koncsos, L., 1990. Sediment resuspension and its impact on changes of algal biomass. Doctoral thesis, Technical University of Budapest (in Hungarian).

Luettich, R.A., Harleman, D.R.F. and Somlyódy, L., 1990. Dynamic Behavior of Suspended Sediment Concentrations in Shallow Lake Perturbed by Episodic Wind Events. Limnol. Oceanogr., 35: 1050–1067.

Orlob, G.T. (Editor), 1983. Mathematical Modelling of Water Quality: Streams, Lakes and Reservoirs. Wiley, Chichester, 518 pp.

Shanahan, P., Harleman, D.R.F. and Somlyódy, L., 1986. Wind induced water motion. In: L. Somlyódy and G. van Straten (Editors), Modelling and Managing Shallow Lake Eutrophication, with Application to Lake Balaton. Springer, Berlin, pp. 204–255.

Somlyódy, L., 1982. Water quality modelling: a comparison of transport-oriented and ecology-oriented approaches. Ecol. Modelling, 17: 183–207.

Somlyódy, L., 1983. Input data uncertainty and parameter sensitivity in a lake hydrodynamic model. In: M.B. Beck and G. van Straten (Editors), Uncertainty and Forecasting of Water Quality. Springer, Berlin, pp. 129–56.

Somlyódy, L., 1986. Wind induced sediment resuspension in shallow lakes. In: Proc. Int. Conf. on Water Quality Modelling in the Inland Natural Environment, 10–13 June 1986, Bournemouth, UK. BHRA Fluid Engineering Centre, Cranfield, Bedford, pp. 287–298.

Somlyódy, L. and van Straten, G. (Editors), 1986. Modelling and Managing Shallow Lake Eutrophication, with Application to Lake Balaton. Springer, Berlin, p. 386.

Steele, J.H., 1962. Environmental control of photosynthesis in the sea. Limnol. Oceanogr., 7: 137–150.

Straskraba, M., 1976. Development of an analytical phytoplankton model with parameters empirically related to dominant controlling variables. In: R. Glaser, K. Unger and M. Koch (Editors) Umweltbiophysik. Akademie Verlag, Berlin, pp. 33–65.

Štraškraba, M. and Gnauck, A., 1985. Freshwater Ecosystems. Modelling and Simulation. Elsevier, Amsterdam, p. 309.

Thomann, R.V. and Mueller, J.A., 1987. Principles of Surface Water Quality Modelling and Control. Harper and Row, New York, p. 644.

van Straten, G., 1980. A note on the effect of light penetration fluctuations on algal growth in Lake Balaton. In: G. van Straten, S. Herodek, J. Fischer and I. Kovács, (Editors), Proc. Second Joint MTA/IIASA Task Force Meeting on Lake Balaton Modelling, Vol. I, pp. 176–194.